A Critical Update of Experimental Techniques of Bulk and Interfacial Components for Fluid Characterization with Relevance to Well Fluid Processing and Transport.

Sébastien Simon, Jost Ruwoldt, Johan Sjöblom

Ugelstad Laboratory, Norwegian University of Science and Technology, 7491 Trondheim, Norway

Abstract:

The present article reviews techniques to address central flow assurance and separation issues. It is our purpose to update the need for extended information in order to draw adequate conclusions about the reason for irregularities in production and how this is related to individual components or fractions in the crude oil. Our intention is to show that the mass related analysis (such as SARA, MS etc.) are insufficient for a validation of the early stage predictions concerning irregularities. The review introduces a set of new characterization and fractionation techniques such as interfacial rheology, SANS, and NMR, where the central theme is the functionality of the components and not just their mass. Two crude oil-related issues are addressed: Wax precipitation and deposition, and crude oil/water resolution. First, bulk techniques to characterize wax precipitation are reviewed. The influence of the chemistry of other crude oil components (asphaltenes) and wax inhibitor on the precipitation is highlighted. Secondly, in aqueous systems, interfacial w/o conditions are important for the stability of dispersed systems. Asphaltenes have a crucial and important role in the stability of crude oil emulsions. Here special attention is directed to properties like interfacial viscosity and elasticity as well as the adsorbed layer structure determination. Small molecular changes in these properties will have dramatic influence on the stability of the heterogeneous systems. A good example is inhibitor functionality.

Keywords: Wax; Asphaltenes, Experimental characterization; Flow assurance; Separation; Deposition; Interface.

Table of Contents

List of Abbreviations:

ADSA: Axisymetrical Drop Shape Analysis

AFM: Atomic Force Microscopy

APCI: Atmospheric Pressure Chemical Ionization

APPI: Atmospheric Pressure Photoionization

ASTM: American Society for Testing and Materials

Bo: Boussinesq number

Ca: Capillary number

CPM: Cross-Polarization Microscopy

D: diffusion coefficient

DBE: Double-Bond Equivalent

DLA: Diffusion Limited Aggregation

DOSY: Diffusion-ordered Spectroscopy

DPT: Drop/bubble Profile Tensiometry

DSD: Droplet Size Distribution

DSC: Differential scanning calorimetry

DWR: Double Wall Ring

EOR: Enhanced Oil Recovery

E': elastic dilatational modulus

E'': viscous dilatational modulus

E-SARA: Extended-SARA

ESI: Electrospray ionization

FT- ICR MS: Fourier transform ion cyclotron resonance mass spectrometry

FTIR: Fourier transformed-infrared spectrometry

G': Storage Modulus

G'': Loss Modulus

GC/FID: Gas Chromatography/Flame ionization detector

GC/MS: Gas Chromatography/Mass Spectrometry

HT-GC: High Temperature-Gas Chromatography

IAA: Interfacially Active Asphaltenes

IFT: Interfacial Tension

ITC: Isothermal Titration Calorimetry

LVDT: Lucassen and van den Tempel

MD: Molecular Dynamics

NA: naphthenic Acids

NIR: Near-Infrared

NMR: Nuclear Magnetic Resonance

PPD: Pour Point Depressant

QCM-D: Quartz crystal microbalance-Dissipation

RA: Remaining Asphaltenes

Re: Reynolds number

SARA: Saturates, Aromatics, Resins, Asphaltenes

SANS: Small Angle Neutron Scattering

SAXS: Small Angle X-ray Scattering

SDT: Spinning Drop Tensiometer

ST: Surface Tension

VPO: Vapor Pressure Osmometry

WAT: Wax Appearance Temperature

We: Weber number

W/O: Water/Oil

1   Introduction

All characterization of crude oils are central for mitigation and remediation operations of irregularities in the oil processing. Characterization will provide information on the formation conditions (P, T, pH…) and properties (rheology…) of inorganic and organic deposits such as scales, asphaltenes, waxes, calcium naphthenate deposits as well as the stability and stabilization mechanism of crude oil emulsions. The result of a thorough analysis will serve as basis for decisions concerning important processes like transport and production of the well-fluids. Different phenomena like organic and inorganic deposits, precipitation and emulsion formation will cause severe operational problems and are all dependent on the compositional map of the crude oils[1]. As such an early stage characterization will influence the whole development and planning of oil-bearing formations. Obviously, process engineers rely on these results for very far-reaching decisions for the whole infrastructure and future operation of the field.

The characterization of crude oils has undergone considerable modernization and update during the last 10 years. A traditional and conservative way to describe the state of a crude oil has always been to relate the crude oil behavior to the mass of the components. This is also the basis of the most wide-spread characterization which is the SARA analysis where the fractions of saturates, aromatics, resins and asphaltenes are given as a background for an understanding of crude oil behavior[2, 3, 4, 5]. The need for an update of this classical approach is seen from a comprehensive challenge of not only the mass of the components but also their functionality, a field where the SARA completely fails. The SARA reports the precipitation of asphaltenes prior to any other analysis of the remaining components, which are determined chromatographically. This can have its relevance for a description of saturation and aromaticity. However, recent research has emphasized how small amounts of chemicals either already present in the crude oil or added as inhibitors of the type demulsifiers and defoamers to the systems can alter fundamental properties of the crude oils. Under these new conditions we discuss mass changes in the order of ppms, which are by far too small to be detected by any conventional, analytical technique. The only way to identify the influence of these additives is to follow the change in the surface / interface properties both mechanical and chemical. Obviously, a modern laboratory for crude oil research must cover both bulk and interfacial aspects of the crude oils for both academic and industrial clients.

The purpose of this review is to give an update of some existing modern experimental techniques and their complementary information for a better understanding of the crude oil state. This will allow to avoid irregularities at an early production state Special understanding is directed towards the behavior of small amounts of inhibitors.

2 Important crude oil components and their chemistry

A crude oil consists of thousands and thousands of individual components. Hence a complete characterization of all these components will render an impossible challenge for the laboratories in the field. Despite of this background mainly one technique has been developed to give an extensive picture of the individual components, i.e. FT-ICR MS.

Other techniques mainly aim at characterization of classes of components determining the bulk and interfacial properties of crude oils. We restrict our description here to involve waxes, asphaltenes and (briefly) special species of naphthenic acids.

2.1 Techniques for identification of all components in the crude oils – Petroleomics.

This section presents a brief overview of the Fourier transform ion cyclotron resonance mass spectrometry(FT- ICR MS) technique.

FT-ICR MS is a powerful analytical technique with excellent resolution that allows to determine the elemtal composition of mixtures. It has been applied to analyze many oil-related compounds: Naphthenic acids[6], nitrogen-bearing compounds[7], calcium and sodium naphthenate deposits[8, 9], asphaltenes and so on. In a single analysis, the composition of thousands of species can be determined. For instance, Qian et al.[10] have identified 3000 nitrogen-containing aromatic compounds from a single FT- ICR MS spectrum in extra heavy oils.

FT- ICR MS that allows to determine the elemental compositions ($C_cH_hN_nO_oS_s$) as well as the double-bond equivalents (DBE), i.e. the number of rings plus double bonds to carbon, of molecules present in crude oil[11, 12]. Once these species are identified, different types of plots are built to visualize the main characteristic of the samples:

- Heteroatom class distribution. This bar plot represents the abundance for every class i.e. all species with the same $N_nO_oS_s$ composition (ex NO, SO_2...).
- For a specific heteroatom class, the double-bond equivalent can be plotted as a function of the carbon number.
- Finally, the van Krevelen diagrams[13] can be built. They represent the variations of H/C ratio as a function of X/C ratio with X: a heteroatom (N. O, or S).

One of the problems with the method is the quantification. The signal measured by the detector is function of the ionization yield of the specie, which depends on its polarity and the ionization technique[14]. Electrospray ionization (ESI) is particularly efficient to ionize polar constituents with high heteroatom content. Atmospheric pressure chemical ionization (APCI) and atmospheric pressure photoionization (APPI)[15, 16] ionize low polarity compounds, such as hydrocarbons. The choice of the mode of detection (negative or positive mode) will also combine to the complexity of the analysis. In conclusion, the choice of the ionization technique will determine which species are analyzed and detected. Hence, the sample preparation is crucial for the success of the FT- ICR MS analysis.

Alternatively, FT-ICR MS has also been directly applied on samples with no prior separation or fractionation. Even if this has the advantage of simplicity, it can bring some bias to the analysis. For instance, if some components are more easily ionizable, this can mask the presence of other components. This has been shown for the case of asphaltenes: Chacón-Patiño et al. have found that co-precipitated maltenes from asphaltenes in n-heptane solution need to be removed to enable identification of abundant archipelago asphaltenes[17]. In the case of naphthenic acids (NA), Rowland et al. have reported that low molecular weight NA are preferentially ionized and suppress the ionization of the highest masses. Consequently, they have developed a method to separate NA into fractions of increasing molecular weight before their characterization by ESI FT-ICR MS[18].

The development of FT-ICR MS is the background for the concept of "petroleomics"[12, 19]. Petroleomics, in parallel to Proteomics in the field of proteins, aims to determine the relationship between the chemical composition of an oil and its properties. Currently, to the best of our knowledge, the high ambitions of the FT-ICR MS have not been successfully met so far.

In conclusion, FT- ICR MS is a technique of choice when the knowledge of the molecular composition of an oil sample is required. However, its implementation (preparation of the sample, ionization and detection modes, …) will influence the types of compounds that will characterized.

2.2 Techniques for identification of central bulk components and their chemistry.

2.2.1 Paraffin waxes

2.2.1.1 Presentations of waxes

Paraffin waxes are an important class of the bulk species and very central in determining the flow properties of the crude oils. Indeed, waxes can deposit on pipeline walls restricting flow as well as increase the viscosity of the crude oil fluid when they precipitate due to temperature and pressure changes. The waxes are composed of mainly straight chain alkanes (n-alkanes) with some branched

and cyclic elements (iso- and cyclo-alkanes). Waxes belong to the high molecular end of crude oils components. They can contain molecules up to one hundred carbon atoms (C_{100}) and more. The lower limit is set to an interval from 16 to 20 carbon atoms, depending on definition of the author[20, 21, 22]. A traditional way to categorize paraffin waxes is according to their exhibited crystal structures, i.e. straight chain, low molecular weight waxes forming larger plate- and needle-shaped crystals are considered macrocrystalline and waxes rich in cyclo- and iso-alkane derivates exhibiting smaller and compact crystal shapes are referred to as microcrystalline. Both of these types can and will cause irregularities due to temperature gradients or production stop. The large flakes and needle-shaped crystalline structures in macrocrystalline waxes are especially prone to three-dimensional interlocking, which strongly influences waxy gelling and other flow properties of the waxy oil. The microcrystalline category will result in smaller and amorphous particles with lower gel strengths. Authors recently found that with increasing ratio of iso-alkanes, the transition between macro- and microcrystalline wax does not follow a gradual but rather an immediate change between the two states[23]. Obviously, the final structure is not only depending on molecular composition but also on the kinetics behind the cooling process and other indigenous components that can influence the wax crystallization process. These substances shall be discussed in detail in section 3.1.3.2.

2.2.1.2 Determination of crude oil wax content

In analogy to asphaltenes, which are defined in terms of their solubility properties, procedures exist for solvent dewaxing that measure the total wax content. A definition of such procedure was introduced by Burger et al.[24], which is often referred to as the *acetone precipitation method* and was later stated by UOP method 46-64. Crude oil is first mixed with petroleum ether, diluted with an excess of acetone and cooled at -20 °C. The solid wax crystals are separated via filtration and quantified gravimetrically. Modified versions of this method were subsequently published utilizing e.g. cooling at lower temperatures[22]. Moreover, sample purification via adsorption on a packed bed column prior to wax crystallization was stated e.g. in the Chinese Petroleum Test Standard SY/T 7550–2000[25]. The equivalent European standard, EN 12606-2, uses a mixture of ethanol and ether to precipitate waxes at -20 °C. However, little to no effort has been made recently for improving these procedures, as distinguishing waxes based on solubility properties has severe limitations. The amount and selectivity of precipitated components may depend on both solvent and separation temperature and according procedures often exhibit an inherently large scattering with relative error margins of 10 % and more. In addition, co-precipitation of other components than wax can be invoked, which would require e.g. careful removal of asphaltene and resin compounds prior to dewaxing.

Procedures based on gas chromatography (GC) can provide both the carbon number distribution and the total wax content as cumulative sum of the latter. By the use of predictive models, these data may also allow the calculation of wax appearance temperature (WAT)[26]. The challenge in such an approach lays in the fact that the higher molecular weight waxes found in crude oil can exceed the operating conditions of regular GC. Even with adaptations such as high temperature GC/FID, the quantification of alkanes with carbons number of 100 and larger is considered difficult. In addition, *iso*-alkanes often have a broad spanning range of elution times, which makes accurate identification difficult. A recent development was the introduction of two-dimensional GC/MS, which allows separation of components e.g. based on boiling point (dimension one) and polarity (dimension two). Authors have successfully applied this technique to characterize certain crude oil fractions[27], however, reliable quantification and the high temperature spectrum necessary for the analysis of high molecular weight waxes is still lacking.

Proton (H^1) nuclear magnetic resonance (NMR) is exploiting the difference in time scale of solid and liquid phase signal decay after excitation[28]. In this form, NMR technique has been used for about three decades to quantify the amount of solid wax in a specimen. Recently, a new approach was made by basing quantification on only the contributions from the liquid phase while using deuterated solvent[29]. This approach has the advantage of improved instrument sensitivity at the wax crystallization onset. The requirement for deuterated solvent, however, makes it impossible to use real oil samples, and so this approach is limited to more fundamental studies involving model systems. Another method was developed for proton NMR, which utilizes differences in the chemical shift spectra of methylene groups[30]. In this method, the authors measured CH_2 and CH_3 functional groups, and derived an empirical correlation to predict the total wax content.

Differential scanning calorimetry (DSC) can also be used to determine the amount of crystallized wax, as the thermal signal recorded in DSC corresponds well to the phase transition heat of paraffin wax[22]. Chen et al. have published an empirical equation that relates the integrated DSC heat signal with the total wax content as determined by acetone precipitation method[25]. Recent development in this area includes the work of Coto et al., who developed an iterative procedure to derive the paraffin carbon number distribution from the DSC heat signal[31].

In Fourier transformed-infrared spectrometry (FTIR), the absorbance band around $735 - 715$ cm^{-1} changes with the occurrence of a solid wax phase[32]. Similar to NMR technique, this can be used to measure the total wax content after cooling to a sufficiently low temperature, at which approximately all wax has precipitated.

A comparison of different techniques for determining crude oil wax content has been done e.g. by Robustillo et al.[33].

2.3 Techniques for identification of central interfacially active components and their chemistry.

2.3.1 Definition of asphaltenes

Asphaltenes can be detrimental in oil production since 1) they can precipitate and form solid deposit due to pressure and temperature changes or when crude oil is mixed with another fluid; 2) asphaltenes can also stabilize emulsions, impacting oil-water separation. A conventional and rational definition of asphaltenes is a fraction of the crude oil insoluble in n-alkanes (like n-heptane, n-hexane and n-pentane) but soluble in aromatic solvents like toluene[1, 34]. Already the convention says that this fraction is poorly defined and suffers from a wide polydispersity. Literature reports a diversity of structural proposals to describe the asphaltene molecule. Two often quoted suggestions are reported as the archipelago and the continental model[35], respectively. Both models describe a network of polycyclic aromatic hydrocarbons and saturated hydrocarbon chains. The structures also contain heteroatoms like oxygen, sulphur and nitrogen[36, 37] together with metal compounds nickel, vanadium and iron. Typical for the continental structure is condensed region in the centre of the molecule where polycyclic aromatic hydrocarbons reside. The structure is completed by different polar molecules like acidic groups attached to the central moieties. In the archipelago model the lack of a large centre part of polycondensed species and more of, as the name says, attached smaller ring and chain combinations to form the island-like structure.

Two peculiar properties of asphaltenes need to be presented:

-Asphaltenes adsorb at the oil/water interface stabilizing crude oil emulsions. Since asphaltenes lack the traditional surfactant-like structure, a central question is their interfacial activity[38]. The key to an understanding of this behavior is in the bulk solubility.

-Asphaltenes self-associate in bulk solution and form nanoaggregates. Predominating forces in the interaction with other molecules are pi-pi interaction leading to a molecular stacking, van der Waals interaction originating from the hydrocarbon chains and hydrogen bonding leading to acid-base complexes[39, 40, 41]. All these forms of molecular interplay explain the interaction patterns in bulk solutions with the asphaltene molecules. The strong asphaltene-asphaltene interaction gives rise to aggregates from nanoaggregates upwards which will deposit at the w/o interface or precipitate in solution due to insolubility.

The complex chemistry of asphaltenes makes the understanding of the molecular origin of their properties difficult. In order to reduce asphaltene chemical complexity, two approaches have been used:

-The investigation of simple components, so-called asphaltene model components, capturing the essential features of the asphaltene behavior.

-The fractionation of asphaltenes.

These two methods are presented in the next two sections.

2.3.2   Asphaltene Model Compounds

The chemistry and properties of asphaltene model compounds have been recently reviewed[42]. Only the main aspects are presented and discussed in this section.

As pointed out in section 2.3.1, asphaltenes are strongly polydisperse in structure, chemical functionality, and molecular weight. Consequently, it is difficult to build up structure-property relationship. Nonetheless, several methods have been developed with the aim to develop such relationships; among them petroleomics thanks to resolving power of FT-ICR MS. Other possibilities consist to simplify and rationalize the structure of the sample to be analyzed. Either asphaltenes can be fractionated to obtain less polydisperse fractions or asphaltene model components can be synthesized and analyzed. These model compounds are molecules considered to have a structure similar to "average" asphaltene molecules. By varying their structure in a controlled way, the influence of chemical parameters on the resulting properties can be determined.

Different classes of asphaltene model compounds have been studied reflecting possible variations in asphaltene structure:

- Derivatives of pyrene[43].
- Pyrene derivatives of 2,2'-bipyridine[44].
- Hexabenzocoronene[45].
- The biomarker 5α-cholestane, covalently fused to a range of substituted benzoquinoline groups[46].
- Derivatives of polycyclic aromatic hydrocarbon compound Violanthrone-78[39].
- Perylene-based model compounds[47].

These model compounds have allowed to probe various properties of asphaltenes both in bulk and at the liquid-liquid and liquid-solid interfaces.

- The self-association properties in bulk of derivatives of pyrene and pyrene derivatives of 2,2'-bipyridine were compared with asphaltenes[43, 44]. The aggregation number of these model compounds in o-dichlorobenzene and toluene, measured by vapor phase osmometry, are much lower than extracted asphaltenes. These model compounds do not aggregate or form only dimers and, therefore, lack key features to reproduce asphaltene self-association properties. Hexabenzocoronene[45] was also studied, and it was found that, here also, this molecule forms dimer.
- The cracking and coke formation of 5α-cholestane derivatives[46] and pyrene derivatives[48] were characterized to understand the thermal behavior of asphaltenes.
- Perylene-based model compounds were studied to understand adsorption behavior of asphaltenes at the water-oil interface and the stability of crude oil emulsions[49, 50, 51]. The results have shown the importance of ionized carboxylic acid function.
- Perylene-based model compounds were also studied by calorimetry to understand the interactions between asphaltenes and solid surfaces[52].
- Finally, asphaltene model compounds were studied by molecular modeling to understand asphaltene's self-association and adsorption at the water-oil interface. Derivatives of Violanthrone-78, perylene-based model compounds, as well as structures representing continental and archipelago asphaltenes were considered[39, 53].

In conclusion, asphaltene properties can be mimicked by rather simple organic molecules. However, polydispersity should be considered in a subsequent set.

2.3.3 Techniques of fractionation.

Another possibility to reduce the complexity of asphaltenes and establish correlation between chemical functionalities and key crude oil properties is to fractionate asphaltenes. This approach has been implemented in the last decades mostly using various solvents or mixture of solvents to precipitate different subfractions of asphaltenes. This approach has allowed to show the asphaltene sub-fractions present different bulk and interfacial properties[54, 55].

Recently, Qiao et al.[56] have argued that it would more informative to classify asphaltene fractionation according to their problematic properties i.e. their adsorption profile instead of their solubility. Consequently, they introduced the concept of Extended-SARA (E-SARA), which consists to separate asphaltenes based on their adsorption at oil–water and oil–solid interfaces. The characterization of fractions obtained by this approach allows to identify the key chemical functions responsible for adsorption of asphaltenes at oil-solid and oil-water interfaces. The principle of fractionation for E-SARA is presented in Figure 1.

The E-SARA concept applied to the oil-water interface can be illustrated by the study of Yang et al.[57]. They have fractionated asphaltenes based on their affinity to the toluene-water interface. They recover the asphaltenes present at the surface of water droplet (fraction named interfacially active asphaltenes (IAA)) and remaining in the toluene supernatant phase (remaining asphaltenes (RA) fraction). The analysis of the IAA and RA fractions by electrospray ionization mass spectrometry,

elemental composition, FTIR, ^{1}H and ^{13}C NMR have allowed to construct average molecular representations of IAA and RA molecules and study them by molecular dynamics (MD) simulation[58].

Concerning the adsorption at oil-solid interface, Subramanian et al. have developed a method to fractionate asphaltenes into three fractions using calcium carbonate particles and different solvents[59, 60, 61]. It was found that asphaltene sub-fraction irreversibly-adsorbed on calcium carbonate, contained a higher content of carbonyl, carboxylic acid or derivative groups. It was also showed by isothermal titration calorimetry (ITC), Diffusion-ordered Spectroscopy (DOSY), and Quartz crystal microbalance (QCM-D) that this fraction has a significantly higher tendency to self-associate and form larger aggregates in bulk and adsorb more on stainless steel than the other fractions.
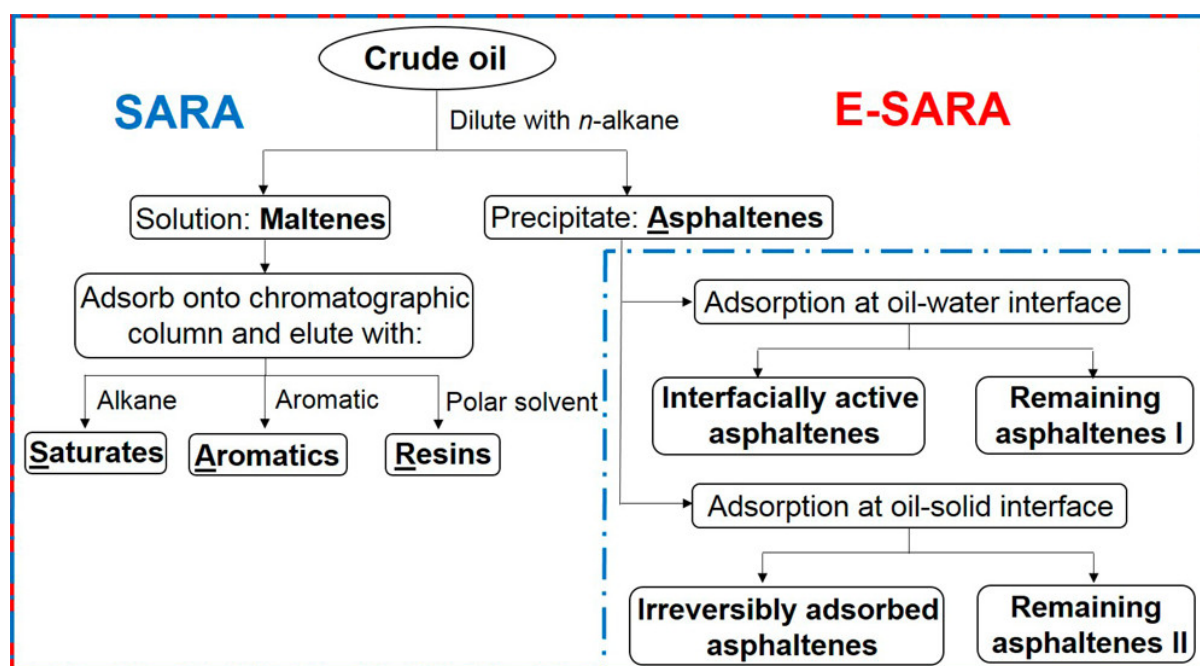
Figure 1: Conventional SARA compared with extended-SARA (E-SARA) analysis according to Qiao et al.[56]. Reprinted with permission. Copyright 2017 American Chemical Society.

3   Characterization of Bulk and Interfacial Properties

3.1   Characterization of Wax Bulk Properties

Crude oil viscosity, i.e. flow-ability, is influenced by various factors, such as temperature and crude oil composition. In terms of flow assurance, crude oil viscosity is also highly dependent on the aggregate and dispersion state of waxes and asphaltenes. When considering bulk properties, waxy gelling or asphaltene and wax deposition are therefore the focus of investigation. Other production issues generally require the presence of a water for gas hydrate or scale formation.

This section only focuses on the influence of wax precipitation on crude oil flow properties. Several different parameters exist, which can be used to describe and quantify states within wax precipitation and deposition. These include the wax appearance temperature (WAT), pour point or gelation point,

crude oil viscosity, waxy gel strength, and wax deposition rate, which will be discussed in detail further below.

The material is arranged in the following way:

-First, basic rheology terms are presented and discussed.

-Second, the characterization of wax precipitation and crystallization is discussed (section 3.1.2.1: onset of crystallization i.e. WAT then section 3.1.2.1: morphology of wax crystals).

-Then the consequences of wax crystallization on crude oil flow are presented (section 3.1.2.3 and 3.1.2.4 on oil viscosity and gelation and section 3.1.2.5 on wax deposition).

-Finally, the influence of other components on wax crystallization is presented in section 3.1.3.

3.1.1 Terminology in Rheology

Several basic rheology terms, used in the subsequent sections, are summarized below.

Viscosity η, one of the most central parameters in rheology, is a measure of a resistance of a fluid to flow, considered as fluid friction. It is defined as:

$$\eta = \frac{\sigma}{\dot{\gamma}} \qquad (1)$$

With σ: the shear stress and $\dot{\gamma}$: the shear rate, that means the derivative of the strain with time.

The viscosity can be independent or depends on the shear rate:

- If the viscosity is independent of shear rate, the fluid is Newtonian.
- If the viscosity decreases when the shear rate increases, the fluid is shear thinning or pseudoplastic.
- If the viscosity increases with the shear rate, then the fluid is shear thickening or dilatant.

For some systems, a minimum shear stress (the yield stress) must be applied before the fluid can flow. These materials are called Bingham plastic.

Oscillatory rheology tests allow to study the structure of materials. In these tests, a sinusoidal shear deformation (or stress) is applied to the sample and the resultant stress (or strain) response is measured. The stress and the strain vary with the same frequency but with a phase shift (δ)

$$\gamma = \gamma_0 \sin(\omega t), \qquad \text{and} \qquad \sigma = \sigma_0 \sin(\omega t + \delta) \qquad (2)$$

With ω: angular frequency. If $\delta=0$, the material is an elastic solid. If $\delta=\pi/2$, the material is a viscous fluid. Finally, a viscoelastic material is defined as $0<\delta=0<\pi/2$.

Oscillatory tests allow to define the storage modulus G' and the loss modulus G'' from the relationship between the strain and the stress:

$$\sigma = \gamma_0 (G' \sin \omega t + G'' \cos \omega t) \qquad (3)$$

Oscillatory tests are generally performed in the linear viscoelastic regime to avoid disturbing the structure of the material during the test. In this regime, G' and G'' are independent of the strain amplitude.

Other tests, such as relaxation or creep tests, exist to characterize materials. Readers are referred to rheology textbooks for more information[62].

3.1.2 Crude Oil Flow Properties

The flow behavior of crude oil is an important parameter when designing production infrastructure and facilities, as well as when anticipating or mitigating production irregularities. It is therefore central to describe and predict oil viscosity and operating regimes where hindrance of flow might occur.

3.1.2.1 Wax Appearance Temperature (WAT)

The WAT, also referred to as wax precipitation temperature or cloud point, is defined as the highest temperature at which wax crystallization can be measured or observed[63]. Due to this definition, the WAT always resembles an experimental value, which can vary for different experimental conditions[64]. The experimental WAT must be distinguished from the thermodynamic WAT, which describes the thermodynamic solubility limit of paraffin wax in a given solvent. Experimental WAT is therefore expected to be lower than thermodynamic WAT, since a certain fraction of wax has to first precipitate to be detected[22].

The WAT is an important parameter for designing and operating petroleum production facilities, since the WAT serves as a first indicator on production issues due to wax[63]. Over the years, many techniques have been proposed for measuring WAT. Authors have previously grouped these into categories depending on the measuring principle[64, 65]:

(i) Visual detection methods: Cloud point measurements observe crystal occurrence or cloudiness in a liquid specimen[66]. Cross-polarized microscopy (CPM) utilizes that wax crystals can change the axis of rotation of polarized light, enabling light to pass the second polarization filter, which is oriented perpendicular to the first[21, 63].

(ii) Thermal methods: In differential scanning calorimetry (DSC), the difference in heat flow of a sample container and an empty reference container is measured. Exothermic wax crystallization will invoke a peak in the mostly linear heat flow during constant cooling[21, 63].

(iii) Density variation measurements: The phase transition of wax from liquid to solid can be detected as volumetric shrinkage due to the density difference of the two phases[67].

(iv) Viscometry: The sample temperature is lowered while continuously monitoring sample viscosity. The occurrence of solid particles yields a change in apparent viscosity, which can be used to detect the onset of wax crystallization[21, 63].

(v) Mechanical testing: In filter plugging the pressure drop over a filter is monitored while decreasing the sample temperature[26]. Wax crystallization is detected as an increase in pressure drop. Sonic testing on the other hand utilizes the fact that the velocity of sound in a medium changes with the appearance of wax crystals[68].

(vi) Radiometry: In X-ray computed tomography wax crystals can be observed due to a higher density as compared to the bulk liquid[69]. Near-infrared (NIR) scattering is based on the principle that wax crystals can change the scattering of NIR light[70].

(vii) Electromagnetic methods: In NMR, excited hydrogen nuclei in the solid phase exhibit a shorter relaxation time constant upon realigning to an imposed magnetic field than excited hydrogen nuclei in the liquid phase[28].

Cloud point measurements according to ASTM-D2500 belong to the earliest techniques for determining WAT. However, these have been discussed critically due to inhomogeneous sample temperature, inconsistent cooling gradients, and the method of detection, which can be operator biased[65]. More modern techniques therefore provide automated WAT detection and data treatment is usually done post experiment, which improve reproducibility. CPM technique has also been operator biased in the past, but recent developments towards automatization have been made, e.g. by capturing an image series to do offline WAT assessment[64] or by measuring the total light output as an indicator for wax crystallization[71]. For a long time, CPM has been regarded as the most accurate technique for WAT determination, as a smaller portion of wax has to crystallize for detection than e.g. in DSC or viscometry[22, 26]. However, most studies on WAT method comparison agree that no technique is overall dominant in terms of sensitivity[26, 72, 73, 74]. A recent method comparison has suggested that advances in microcalorimetry and rheometer technology have surpassed CPM technique in sensitivity[75]. Indeed, recent developments such as micro-, nano- and modulated DSC have yielded improvements in instrument sensitivity[76]. Here, the application of cooling intervals in combination with isothermal segments (StepScan) can be used to reduce super cooling effects[77]. However, parameters such as wax composition and cooling rate also have profound impact on the experimental WAT[64], which is often neglected. As a general rule, the WAT values obtained by different techniques or settings are less ambiguous, if the wax crystallization event is starting at a high rate, i.e. a large portion of wax is crystallizing immediately at WAT.

3.1.2.2 Characterization of Wax Crystallization

Wax crystal morphology is a central parameter to qualitatively evaluate wax crystallization. Cross-polarized microscopy (CPM) has traditionally been used for this purpose[63]. In addition, x-ray diffraction can be used to obtain information on the crystalline structure[78]. The two categories macrocrystalline and microcrystalline waxes are distinguished based on crystal shape, but these differences are also mirrored by wax composition e.g. as determined by high temperature gas chromatography (HT-GC) [78, 79]. Such information is useful, as wax crystal dimensions and shape are directly linked to the rheology of waxy gels. Elementary analysis can also be used to characterize the wax fraction, if available in purified form, because H/C ratios below 2 indicate an abundance of cyclic structures and thereby the presence of microcrystalline wax [78, 80]. Mass spectrometry has also been applied to waxes, which can yield information such as the molecular weight distribution[80]. The recently developed Rheocrystal using the Diffusing Wave Spectroscopy principle is a technique that could be applied to study the

crystallization of waxes in crude oil. It has already implemented to characterize model waxes and chocolate[81].

DSC technique is not only instrumental for determining WAT, but also to perform structural analyses of crude oils such as crystalline phase transitions[76]. DSC allows to determine the wax content in oil as well as the amount of wax crystallized with temperature[82]. DSC is not limited to measure crystallization phenomena upon cooling, but can also be used to study thermal decomposition of crude oil at high temperatures[83]. Another development was made by using high pressure DSC, which mimics the conditions during pipeline transport of live crude oils more closely [84].

Thermal gradient quartz crystal microbalance (QCM) and atomic force microscopy (AFM) were adapted to monitor the formation of an incipient wax layer[85].

### 3.1.2.3   Crude Oil Viscosity and Gelation

An immediate flow assurance issue related to wax formation is the increase of viscosity. At temperature of above WAT, most crude oils, despite their enormous compositional complexity, behave like simple Newtonian liquids. To describe the viscosity change upon cooling, Arrhenius type temperature dependency is often used, but more complex models have also been published[86]. Precipitated wax exhibits a pronounced effect on the viscosity and rheological behavior of these oils. The presence of solid particles in the fluid increases the viscosity. At low temperatures where wax precipitation is most extensive, the oils typically behave like pseudoplastic or viscoplastic fluids[87]. An increase in viscosity will dramatically reduce pump efficiency in conjunction with reductions in flow rate, increase of power consumption, and eventually increase in cost.

Flow properties are most often measured in a rotary rheometer. Such methodology has been established for decades and recent advancements include mainly improved instrument sensitivity, which has enabled for example the first correct depiction of the stress-strain progression during waxy gel breakage[88]. Cone and plate geometries are widely used due to easy handling and uniform shear distribution within the sample. Surface roughness of the employed geometry has been pointed out as a crucial parameter to avoid wall slip. Cylindrical Couette geometries, such as bob-cup or double gap, have also proven to be robust designs, which are especially suitable for working with dispersions. In addition, 4-bladed vane geometries have been used to measure breakage and degradation of waxy gels[89], despite non-uniform shear.

The pour point is often used to describe the loss of oil flow-ability, which is defined as the highest temperature at which the specimen can be observed to flow freely[90]. Manual (ASTM D97 and D5853, ISO 3016) as well as automated standards (ASTM D5949, D5985 and D7346) have been established for this purpose. An advantage is the technological simplicity of the test setups compared to modern rheometers, however, this also entails disadvantages such as low resolution of the manual methods or the lack of a physical relation for the observed pour point. The pour point quantifies wax crystal growth and agglomeration effects that lead to gelling, but at the same time no qualitative statement is made, e.g. in terms of gel cohesion or yield strength. A more refined approach was therefore made by defining the gelation point. Physically, a fluid is defined to have reached the gelation point if steady state shear viscosity is infinite and equilibrium modulus is zero[91]. A directly measurable definition is provided as the intersection of storage modulus G' and loss modulus G'', as shown in Figure 2. Oscillatory gelation point measurements have been used to both study waxy gelling as well as the effect of crude oil indigenous components thereon [92, 93, 94]. If the strain or stress amplitude is low, this

type of measurement shows some correlation with the pour point[95]. It must be mentioned, however, that the strain amplitude is critical. If it exceeds the linear viscoelastic regime, both G' and G'' will lose their physical meaning[96]. High amplitudes on the other hand can be used to mimic the conditions during turbulent pipeline flow [97]. Non-oscillatory procedures for gelation point determination have also been published [98]. In these a sample specimen is subject to constant shear stress and the gelation point is reached when the shear rate reaches zero. The procedures must be used with caution since the sample is subject to extreme levels of strain.
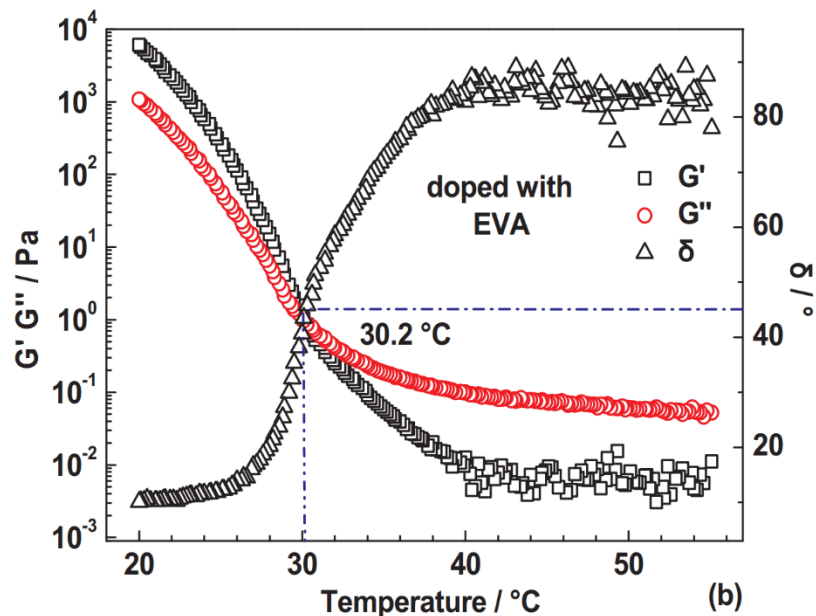
Figure 2: Determination of gelation temperature of a waxy oil using rheology, where G' is the storage modulus and G'' is the loss modulus[99]. See section 3.1.1 for definition of the parameters. Reprinted with permission. Copyright 2018 Elsevier.

3.1.2.4   Waxy Gels

It has been reported that waxy gelling can occur when 1-2% solid wax has crystallized[100]. In addition to detect the onset of waxy gelling, rheometry has also allowed the detailed documentation of flow behavior with importance to pipeline restart, such as gel yielding, creep flow, and waxy gel degradation[101]. Good agreement has been demonstrated between results obtained with a controlled shear rheometer and model pipeline experiments[102, 103]. A new development was made by a rheo-PIV system, which uses flow visualization during controlled shearing of a waxy gel[104]. Surface roughness of the used rheometer geometries as well as thermal history of the sample have shown to greatly affect adhesive and cohesive breakage mechanisms of the waxy gel[104, 105]. Factors such as the radial temperature distribution in the pipeline or shrinkage of the waxy oil during cooling can furthermore yield discrepancies between rheometer and model pipeline experiments, and should therefore be addressed in advance[103].

3.1.2.5   Characterization of Wax Deposition

More applied techniques to investigate wax crystallization with respect to production and pipeline transport include flow loops and cold finger. In a flow loop, hot waxy crude is pumped through a cooled pipe section and the thickness of waxy deposition on the pipeline wall can be determined gravimetrically, via the pressure drop over the pipe segment, measuring the change in oil temperature as waxy deposits can act as insulators, or by laser techniques [63, 106, 107]. A further development was made by equipping a flow cell with a viewing window to monitor the wax deposit buildup in-situ and draw conclusions on the heat and mass transfer boundary layers[108].

The cold finger is made of a cooled cylinder that is immersed in a stirred vessel of hot waxy oil. This has the advantage of simpler experiment setup, however, accurate control of the flow conditions around the wax deposit center is more difficult. More sophisticated designs include the cylindrical Couette device, in which the outer vessel is rotating to induce laminar flow[109]. Another development was made by inversion, i.e. a vessel filled with hot oil that is continuously stirred while wax deposit can form on the outer vessel jacket, which is cooled[110].

A combination of HT-GC and cold finger experiments has given insights into bulk stabilization and aging of waxy deposits[111]. The same approach was also extended to investigate more complex systems including waxes and asphaltenes[109, 112].

3.1.3 Interactions between waxes and other components

3.1.3.1 *Mechanistic Studies of Wax Inhibition*

The study of inhibitor-wax interactions can be grouped into two main approaches: (1) macroscopic bulk effects and (2) molecular interactions. Both approaches are instrumental in providing information on the mechanism of action of wax inhibitors, as well as selection of inhibitor chemistries for efficient wax inhibition. Wax inhibitors are designed to guarantee an unobstructed flow of crude oil even after a considerable amount of wax has crystallized, which is aimed at reducing the pour point temperature. As a result, the terms wax inhibitor and pour point depressant (PPD) are often used interchangeably[113].

Macroscopic effects are manifested in both crystal structure and shape, as well as the flow behavior of a waxy oils with respect to temperature. Co-crystallization in presence of wax inhibitors is targeted to maintain the flow properties of oil by forming compact and small crystals with small interactions. CPM imaging of wax crystal morphology is therefore a commonly used tool to qualitatively assess the efficiency of PPDs[97, 114, 115]. A number of rheometric procedures have been established to probe bulk effects of wax inhibitors, which measure quantities such as crude oil viscosity, gelation temperature, and yield strength of gelled waxy oils[99, 116, 117]. Reduction of pour point also provides a measure for assessing PPD efficiency[118, 119, 120]. WAT depression is a positive side effect that can occur when using crystal modifying polymers[116, 118]. DSC technique has been instrumental not only to map WAT depression, but also to study PPD effect on wax precipitation[99, 121]. As proton NMR has been adapted to quantify the amount of precipitated wax[28], this technique can also be used for assessment of performance of chemical additives[29, 116].

The study of inhibitor-wax interactions on a molecular basis often serves the purpose of uncovering inhibition mechanisms rather than measuring inhibitor efficiency. Simulation techniques, such as molecular dynamics, have been central[122, 123, 124, 125, 126]. Self-aggregation of wax inhibitor polymers has been studied with SANS to map polymer conformation in presence of wax[127, 128]. Isothermal titration

calorimetry (ITC) has been used to measure the interaction strength between PPDs and wax[129, 130]. Moreover, GC technique was applied to quantify inhibitor effect on the depletion of particular *n*-alkanes[116, 118].

3.1.3.2   Asphaltene-wax interactions

Asphaltenes are known to interact with waxes during wax crystallization through a number of mechanisms, even if the asphaltenes have not been destabilized in the crude oil. Studies on asphaltene-wax interactions have frequently employed a combination of either CPM, DSC, rheometry, and pour point tests[94, 115, 119, 131, 132]. Many authors have attributed wax alleviating properties with asphaltenes, which is why these are sometimes also referred to as crude oil indigenous PPDs. Reports can be contradictory at times, since some authors have also attributed aggravating effects to asphaltenes[133, 134] or even stated that there are no synergistic effects between asphaltenes and waxes[135]. The polydisperse nature of asphaltenes is most likely responsible for this[61, 136]. It has been established that asphaltenes can serve as nucleation sites during wax crystallization, which can increase WAT and induce the formation of more finely dispersed wax crystals [94, 119, 133]. Co-crystallization of asphaltenes with waxes has been reported, which further leads to wax crystal distortion and reduced wax oil viscosity[131, 136, 137]. The dispersion state of asphaltenes has been pointed out as a crucial factor for interactions with wax[132, 138].

To study the asphaltene influence on wax crystallization, some authors have isolated asphaltenes from crude oils with different stabilities[131, 134]. Fractionation of previously isolated asphaltenes has furthermore been done by solvent fractionation, in which asphaltenes were dissolved in dichloromethane and sub-fractions were generated by stepwise adding pentane[92, 139]. Another approach was to stepwise precipitate asphaltenes by adding increasing amounts of hexane to crude oil[60, 61]. Moreover, asphaltenes have been fractionated by adsorption on silica gel or calcium carbonate[59, 140]. Authors have concluded that the aliphatic part of asphaltenes is mostly responsible for the interactions with wax[131, 137, 141]. As a result, low polarity and the abundance of alkyl chains were stated to yield better pour point depression, whereas high polarity asphaltenes were reported to interact less with wax[61, 92, 94, 131, 140].

To study asphaltene-alkane complex formation, the retention of long chain alkane compounds on asphaltenes was measured[141]. Asphaltenes and alkanes were mixed in chloroform solvent, equilibrated, filtered and alkane components were subsequently washed off with heptane to be quantified in GC. In a similar approach, asphaltenes and wax were mixed and compacted in solid form, filled into an HPLC column, and subsequently eluted using toluene solvent[134]. ITC has also been used to directly measure the heat of interaction from titrating asphaltene solutions into wax solutions or dispersions[61, 129, 130]. Asphaltenes exhibited similar features as polymeric PPDs, since the interaction heat was considerably larger when crystalline wax was present. Simulations tools, such as diffusion limited aggregation (DLA), are also applicable to study asphaltene behavior during wax crystallization[142].

3.2   Characterization of Liquid/liquid Interfacial Properties

This section focuses on a few techniques implemented to study the adsorption of crude oil components at the oil/water interface. The crude oil components considered are primarily asphaltenes even if ARN tetrameric acid responsible for calcium naphthenate deposition is evoked. The consequences on this adsorption on crude oil emulsion stability is presented in section 3.3.

Properties at the liquid/liquid interface have been traditionally studied by measuring the interfacial tension (IFT) to obtain information on the adsorption of crude oil components. More advanced techniques such as interfacial rheology and Small-Angle Neutron Scattering (SANS) provides a more accurate and detailed description of the interface and its properties.

3.2.1   Interfacial tension measurements

Techniques to determine interfacial tension are well-documented in literature [143], so this part is limited techniques that should be selected for specific information and parameters extractable from the experiments.

3.2.1.1   Measurement techniques

This chapter provides an overview of the traditional techniques.

- Du Noüy ring-Wilhelmy plate force tensiometer: This method allows to determine both surface and interfacial tension by measuring the force to pull a ring or a plate from the interface. This method is easy to implement for accurate equilibrium surface/interfacial tension. With this technique It is difficult to study the adsorption kinetic at liquid/air and liquid/liquid interface and ST and IFT measurement range is standard (down to few mN/m). In conclusion, it is a robust and safe technique for standard measurements. If specific information is required (kinetic, ultra-low IFT), more advanced techniques must be used.

- The sessile/pendant drop techniques. This technique is presented in section 3.2.2.3. It can measure both ST and IFT values like the Du Noüy ring/Wilhelmy plate but, in addition, the kinetics of adsorption can be determined as well as the interfacial dilational rheology properties of the interface. This technique has been implemented to study adsorption of various crude oil components: asphaltenes, naphthenic acids, and production chemicals at different conditions (pH, salinity, and temperature).

- The spinning drop tensiometer. This technique extends the measurement range and allows to determine IFT down to $\approx 10^{-4}$ mN/m. The only applications in petroleum science that requires such a capacity are related to Enhanced Oil Recovery (EOR) and surfactant and alkali flooding. In the SDT, a liquid drop put in a glass tube is filled with a liquid of higher density and brought to rotate around its own axis and its shape is continuously monitored. Provided that the density difference between the two phase is known, the interfacial tension can be calculated[144, 145].

- The maximum pressure bubble tensiometer. This technique can only measure surface tensions and not interfacial tensions. Maximum pressure bubble is particularly adapted to study the first steps of adsorption at water/air interface since it can measure ST down to ca. few milliseconds[146, 147]. The measurement principle is the following: gas bubbles are produced at the tip of a capillary immerged in an aqueous solution. The pressure inside the capillary is measured and at maximum, the surface tension can be determined from the Young–Laplace equation. This technique has been applied

in petroleum science to, for instance, study the adsorption of dissolved components in synthetic produced water to understand mechanisms in the gas flotation process[148].

3.2.1.2   Some information obtainable from ST/IFT measurements

3.2.1.2.1   Adsorption isotherms

ST/IFT values are also used to infer the interfacial composition. Most of the studies are qualitative: the levels of ST/IFT in different systems are compared and some conclusions can be drawn on the composition of the interface. It is more difficult to obtain quantitative values on the interfacial composition due to the extreme complexity of the petroleum systems. We present a method to determine the interfacial composition of a compound from IFT data for model systems (a compound dissolved in a solvent).

The Gibbs equation link the surface excess of component (Γ) to its bulk concentration C (in fact, its activity) at equilibrium[149, 150]:

$$\Gamma = -\frac{1}{nRT} \cdot \left(\frac{\partial \gamma}{\partial C}\right)_{T,P} \qquad (4)$$

With n=1 for nonionic surfactants, R: the gas constant, T: the temperature, and γ: the surface/interfacial tension.

An equation of state must now be introduced to relate the surface excess and the bulk concentration. The Langmuir equation is generally used due to its simplicity, but other possibilities exist:

$$\Gamma = \Gamma_{Max}\left(\frac{K_L \cdot C}{1 + K_L \cdot C}\right) \qquad (5)$$

where Γ_{Max} is the surface excess at saturation and K_L is the equilibrium constant reflecting the affinity for the component to the interface.

Combining the two previous equations gives the Szyszkowski equation:

$$\pi = nRT\Gamma_{Max}ln(1 + K_L \cdot C) \qquad (6)$$

With π: the interfacial pressure=$\gamma - \gamma_0$ with γ_0: interfacial tension in absence of surfactant.

Fitting of interfacial tension as a function of bulk concentration has, for instance, been applied to obtain the adsorption isotherm of asphaltenes at the xylene/aqueous solution (buffer pH=7) by Pradilla et al. (Figure 3).
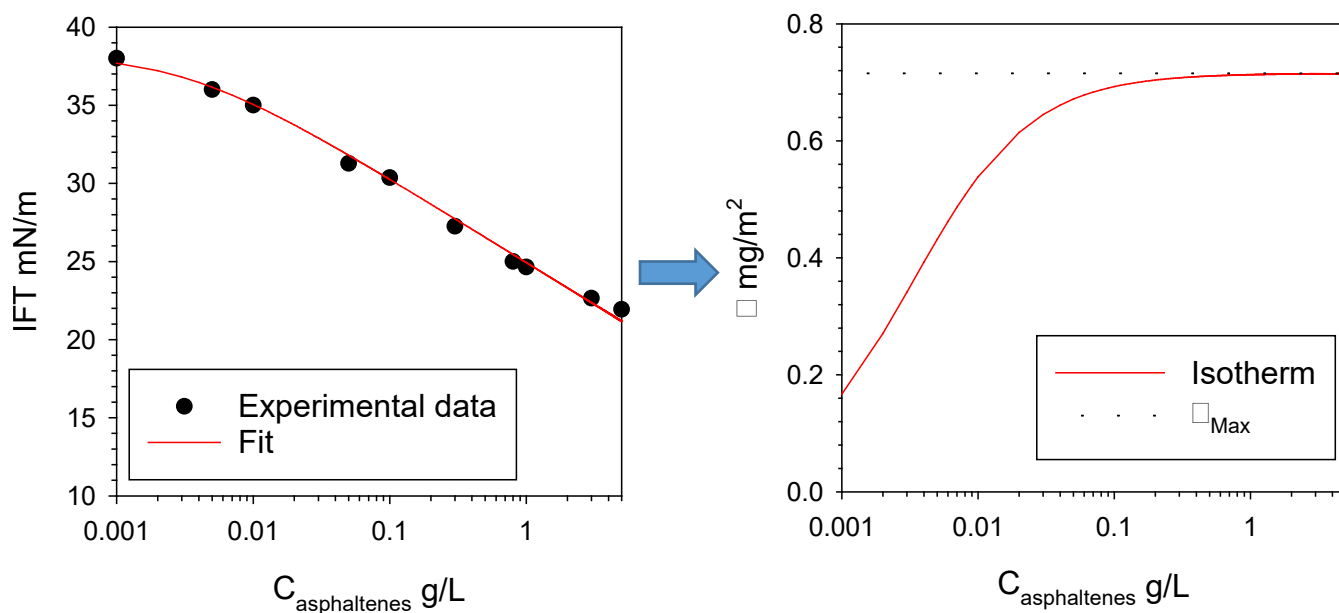
Figure 3: Left: Interfacial tension of asphaltenes at the xylene/aqueous solution (buffer pH=7) interface obtained with a sessile drop tensiometer and fit with the Szyszkowski equation (Γ_{Max} = 9.54 ×10^{-7} mol/m^2 and K_L = 228 m^3/mol) assuming a molecular weight of asphaltenes of 750 g/mol. Right: Calculated adsorption isotherm of asphaltenes. Redrawn from data and analysis by Pradilla et al.[151] with permission. Copyright 2015 Elsevier.

This approach has been used applied to monomeric asphaltenes[151, 152, 153], asphaltene model compounds[51], and naphthenic acids[154].

However, this approach presents some limitations. Especially, it assumes that activity and molar concentration are equal. This is not correct since asphaltenes self-associate[155]. Horváth-Szabó has proposed a method to take into account this point by measuring the solvent activity in asphaltene solutions by vapor pressure osmometry (VPO)[156]. They have applied their method to determine the surface excess of Athabasca asphaltenes.

3.2.1.2.2 Adsorption kinetic

Interfacial tension measurements also allow to study the kinetic of adsorption of components at the oil/water interface. At a fresh interface containing no surfactant, the surface tension is equal to that of pure solvent γ_0. Then, the adsorption of surface-active material will induce a decrease of the surface tension γ until the equilibrium value γ_{eq}. The kinetic gives information on the nature of adsorbing species.

Equations of model adsorption at liquid/air and liquid/liquid interfaces have been reviewed by Eastoe and Dalton[149] and by Chang and Franses[150].

In the models, the surfactant molecules are assumed to diffuse from the solution bulk to a "subsurface", a few molecular diameters below the interface. After the surfactant has diffused to the subsurface it will either directly adsorb at the interface or will pass through a potential barrier before adsorbing and as a consequence the adsorption is delayed. In the first case the entire process is therefore controlled by diffusion of surfactant. The second case is controlled by adsorption and the adsorption barrier.

In the case of diffusion-controlled process, Ward and Tordai have proposed in 1946 an equation linking the surfactant surface excess with time[157]. Two asymptotic solutions can be derived to study adsorption kinetic[158]:

- The short-time approximation, in which we have the following relationship:

$$\gamma = \gamma_0 - 2nRTC_0 \left(\frac{D}{\pi}\right)^{1/2} t^{1/2}$$ (7)

With t: time, C_0: bulk concentration and D: diffusion coefficient

- The long-time approximation when $\gamma \to \gamma_\infty$:

$$\gamma = \gamma_\infty + \frac{nRT\Gamma_{eq}^2}{C_0} \sqrt{\frac{\pi}{4Dt}}$$ (8)

With Γ_{eq}: surface excess at the equilibrium state.

In practice, it is the short-term equation that is mostly used since the long-term version requires values of Γ_{eq}. In addition, generally dilute solutions are analyzed since the first stages of adsorption cannot be captured with tensiometer (pendant drop or maximum bubble tensiometer) if the concentrations are too high: The first measured interfacial tension values are generally significantly lower than γ_0. Then the variations of the interfacial tension are plotted as a function of $\sqrt{t}$ and the diffusion coefficient can be determined from the slope of the linear part of the curve.

This approach has been applied in the case of adsorption of asphaltenes. It was found that this diffusion coefficient is significantly lower than values found in bulk which means that a small fraction of asphaltenes adsorb at the liquid/liquid interface or the adsorption is reaction-limited[151, 159]. In the first approach the interface serves as chromatographic surface. It was also found that adsorption equilibrium of asphaltene is not reached before several hours and sometimes even more. This is attributed to reorganization in the surface plane. This long-term process is generally fitted with phenomenological equations like monoexponential or biexponential ones that are used to compare systems with each other[54, 160].

3.2.1.2.3   Desorption

Finally, Interfacial tension measurements allow to study the desorption of petroleum components once adsorbed at the liquid/liquid interface. This can be achieved by using a sessile/pendant drop tensiometer equipped with a double coaxial capillary system (<u>Figure 4</u>) developed by Ferri et al.[161, 162]. A component is adsorbed at the surface of a droplet. After this, the solution inside the droplet is replaced by flowing pure solvent. By measuring the interfacial tension before, during and after the replacement, desorption can be assessed.

Figure 5 presents the results of desorption of asphaltenes in xylene at the xylene/aqueous solution (buffer pH=7). In this experiment, asphaltene are adsorbed for 1.5 hours without reaching equilibrium which is seen from the continuous decrease of IFT(step 1). The injection of pure solvent starts (equivalent to a flow rate of 0.2 µL/s) and the variations in interfacial tension allow to follow the desorption of asphaltenes (step 2). Finally, after a pre-determined volume is fully replaced (1000 µL), exchange is complete (step 3). The IFT reaches a plateau during the solvent exchange that is intermediate between the value before exchange and the one corresponding to surfactant-free interface. Consequently, there is partial desorption.
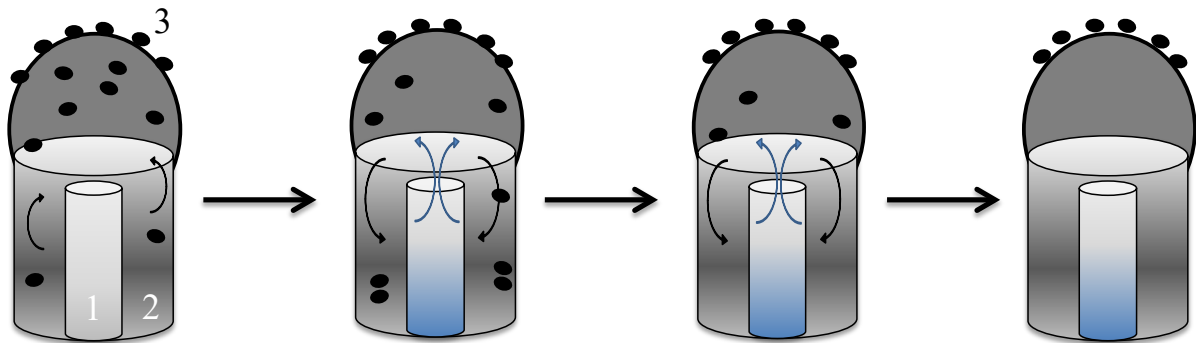
1. Inner capillary.
2. Outer capillary.
3. Oil droplet.

Figure 4: Scheme showing how the desorption process of a surface active molecule can be studied by the injection of a volume of pure solvent in a coaxial double capillary system. The interfacial tensions are determined by sessile/pendant drop tensiometry. Scheme by Pradilla et al.[151]. Reprinted with permission. Copyright 2015 Elsevier.
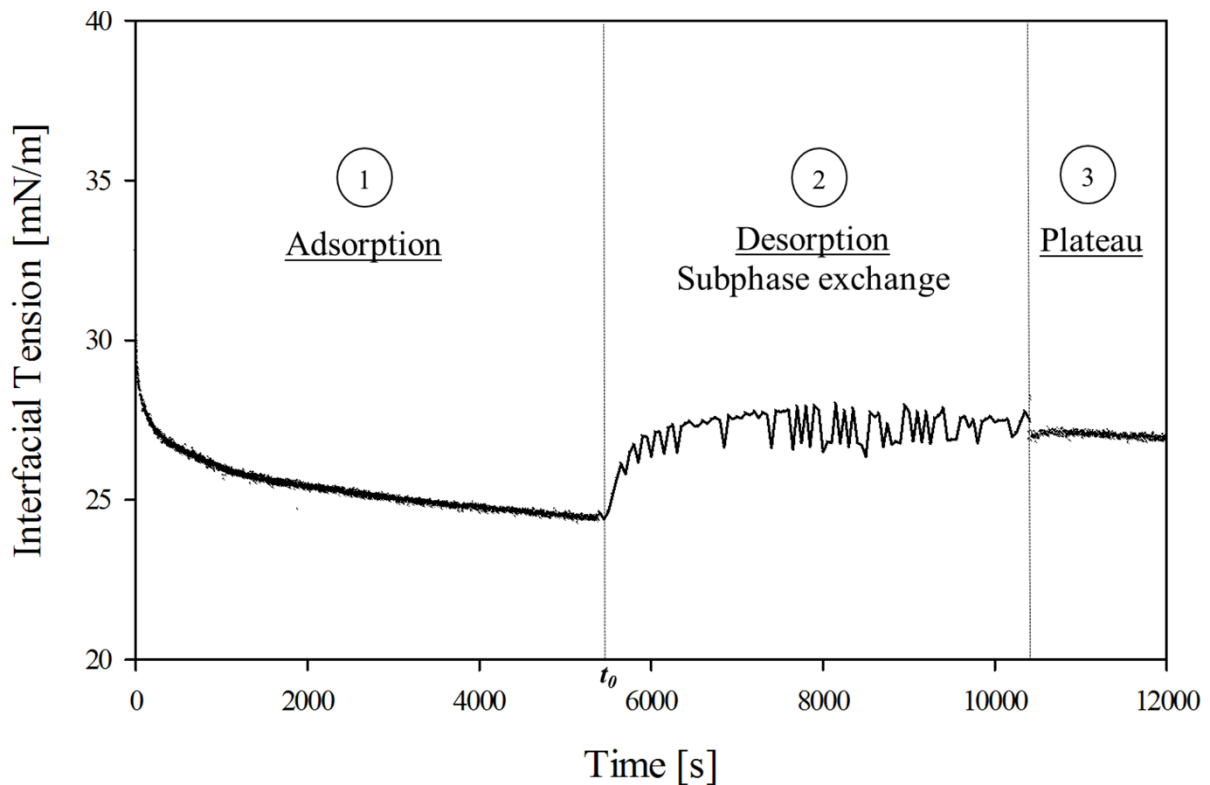
<u>Figure 5:</u> Variations of the interfacial tension during adsorption (step 1) and desorption of asphaltenes by pure solvent (step 2). The flow is stopped in step 3. The conditions are described in the text. After Pradilla et al.[151]. Reprinted with permission. Copyright 2015 Elsevier.

The same co-axial capillary device can also be used to study the desorption or replacement of a component pre-adsorbed at the liquid-liquid interface by a second component. This has been implemented in desorption of asphaltenes by model-demulsfiers[152].

An alternative has been developed by Teclis Scientific (France) to study desorption. This set-up consists of a liquid drop (termed liquid bridge) placed between two vertical capillaries. The interfacial tension is calculated from the shape of the drop. A flow of solvent passing through the drop while keeping its volume constant allows to study the desorption of a component previously adsorbed. This set-up has been applied to confirm that asphaltenes are irreversibly adsorbed at the oil-water interface[159].

3.2.2   Interfacial Rheology

3.2.2.1   Introduction and comparison with bulk rheology

Interfacial rheology, similarly to the classical bulk rheology, is used to determine the response of interfaces against deformations[163]. This approach can be traced back to the 19th century as recalled by

Miller et al. and Masschaele et al.[164] The interest for interfacial viscosity (and elasticity) is due to significant difference from adjacent bulk phase.

Interfacial rheology is frequently used in petroleum science to study interfaces built by asphaltenes. This interest is linked to the visual observation that asphaltenes form a rigid skin at interfaces[160, 165]. Few studies have also been extended to naphthenate systems.

Interfacial rheology can be seen as a 2-dimentional analogue to 3-D bulk rheology, but also presents unique features.

Similar to bulk rheology, interfacial rheology can be divided into sub-classes differing by the type of induced deformation– dilational and shear rheology (Figure 6). The choice of the sub-technique strongly influences the nature of sample to be measured, the information that can be obtained, and the apparatus that needs to be implemented.

- Interfacial shear rheology allows to perform similar tests as the bulk rheology (flow curves, oscillations, creep and relaxation tests[166]), and analysis are similar after decoupling the bulk and interface signals.
- Interfacial dilational rheology tests have differences with bulk rheology since adsorption/desorption of surfactants to/from interface need to be taken into account to explain the results.
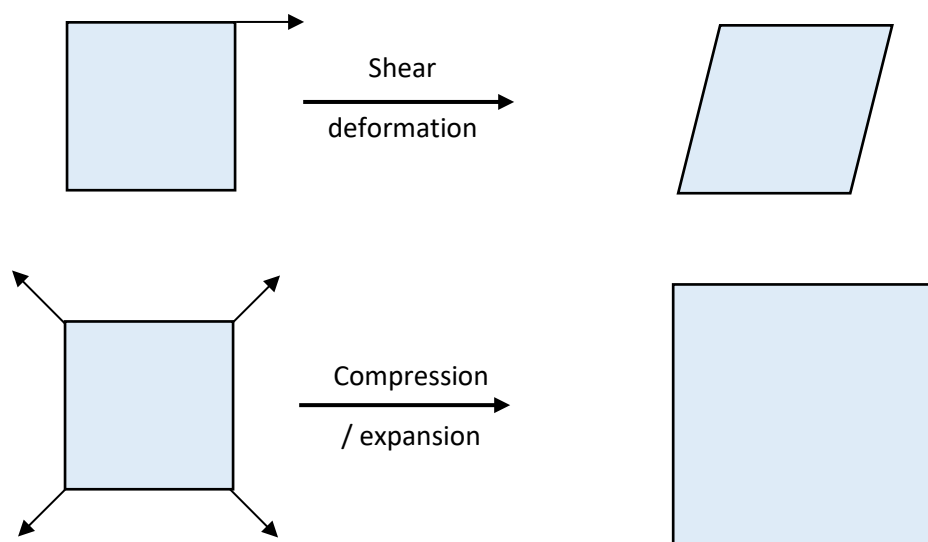
Figure 6: Type of deformations in interfacial rheology. Up: shear rheology; Down: dilational rheology.

These two techniques are presented in detail in the following:

3.2.2.2 Interfacial shear rheology

The shear deformation induces modification of the shape of the interface by keeping the surface area constant[167, 168]. The composition of the interface is constant during the deformation and, consequently, the measured signal only comes from the mechanical properties of the interface. Different geometries and set-ups have been used to measure the interfacial rheology properties of petroleum compounds under shear: biconical disk either linked to a torsion wire or a rheometer has traditionally been used[169, 170, 171] and, more recently, double wall ring (DWR) [172] has been introduced which appears to be more sensitive[173]. Both geometries are presented in Figure 7.
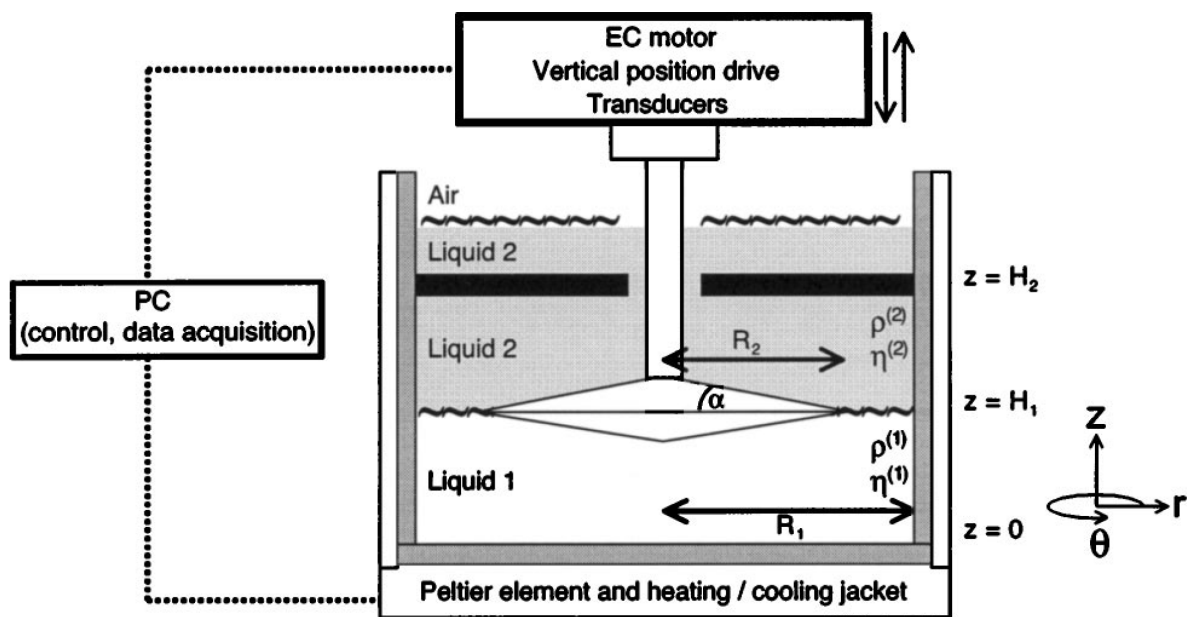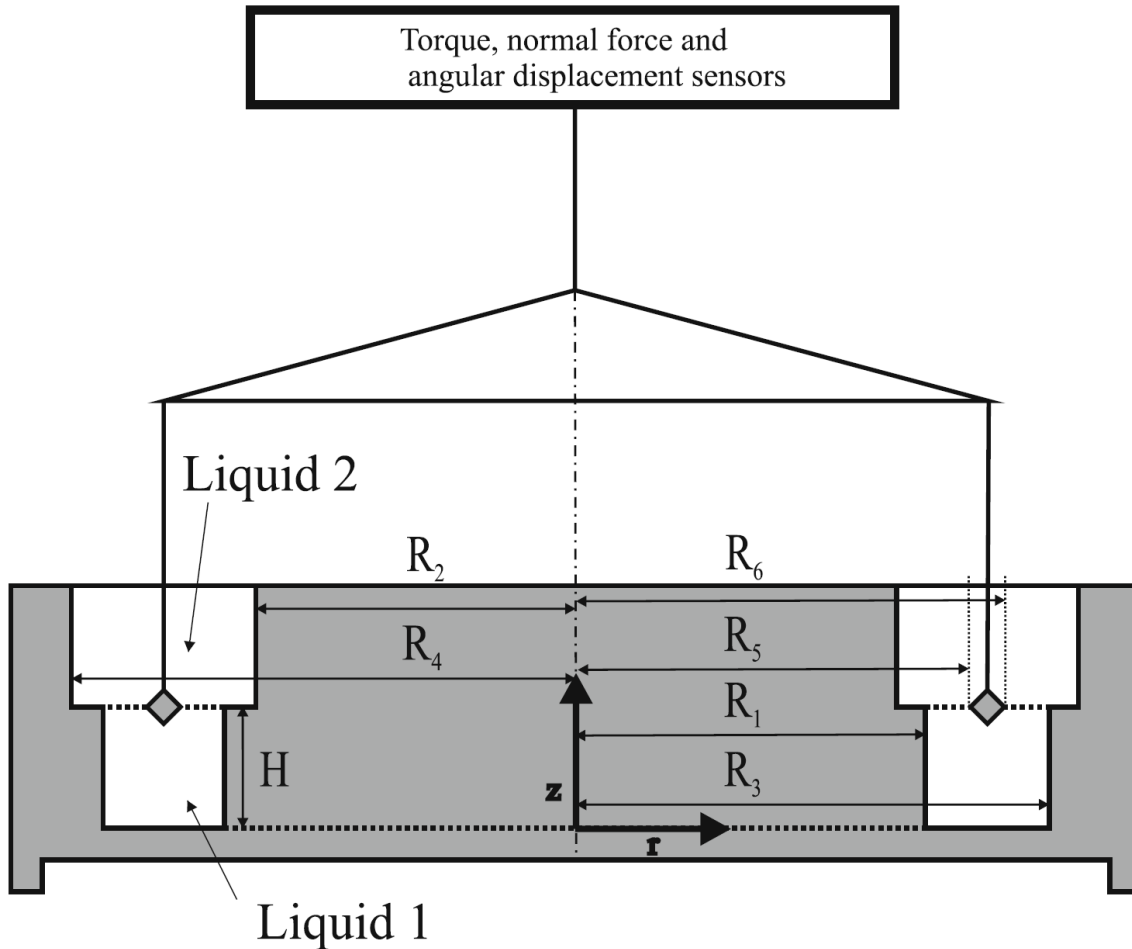
Figure 7: Schematic of a biconical disk (top) and double wall ring (DWR-bottom) geometries. Top by Erni et al.[166]; bottom by Vandebril et al.[173]. Reprinted with permission. Top: Copyright 2003 AIP Publishing; bottom: Copyright 2009 Springer Nature.

A fundamental measurement problem in interfacial shear rheology is the de-coupling between the flow profile at the interface and that in the surrounding bulk phases (subphase). This phenomenon is quantified by the Boussinesq number (Bo) which describes the importance of the surface drag relative to the bulk.

$$Bo = \frac{Surface\ drag}{subphase\ drag} = \frac{\eta_S}{\eta \cdot G} \tag{9}$$

With η_S: interfacial shear viscosity, η: bulk viscosity, and G: parameter dependent of the dimensions of the measurement geometry. The Boussinesq number presents two limiting cases:

- |Bo| >> 1, the interfacial stresses dominate and the surface rheological properties can be easily calculated from the measurements
- |Bo| ≤ 1, the subphase properties are measured
- For intermediate values, bulk phase contributions must be taken into account in the calculation of the interfacial viscosity.

Interfacial shear rheology is not a sensitive technique. Consequently, only systems with significant values of interfacial viscosity can be characterized. In addition, the viscosity of the bulk phases must be kept as low as possible. That is why only model systems composed of crude oil components such as crude oil dissolved in a low viscous organic solvent such as toluene or xylene or crude oil diluted in the same type of solvents[174] have been studied.

Different types of measurements can be performed in interfacial shear rheology: flow tests where interfacial viscosity is measured, oscillations measurements which allows to determine the G'_I and G''_I moduli function respectively of elasticity and viscosity of interface, and creep and creep recovery tests to study the viscoelasticity of the interface. Finally obtained data must be carefully examined to make sure that the measured signal (torque) is higher than the detection limit of the rheometer.

Two types of petroleum systems have recently been studied by interfacial shear rheology: asphaltenes and calcium naphthenates[175, 176, 177].

Asphaltenes at interface have been studied to understand the stability of petroleum emulsions[6, 178]. It was found that the asphaltene layer exhibits mostly elastic behavior ($G'_I > G''_I$). The kinetic of film formation is slow: Interfacial shear moduli increase with time and a progression from liquid-like to solid-liquid behavior is observed[179]. This progression takes several hours and, in some systems, G'_I does not reach constant value even after 1 day[169]. Rheology of asphaltene interface is strongly influenced by the solvent quality: in toluene-alkane solvent, G'_I increases when the aromaticity of the solvent decreases. This is consistent with a concomitant increase of the stability of asphaltene-stabilized emulsions. When comparing asphaltenes from different sources, a good correlation between the stability of emulsion and the shear interfacial modulus G'_I was also found [180].

Finally, the addition of surfactants or demulfiers to asphaltene interface results in the transition from a predominantly elastic to a more liquid-like character[169, 170].

Interfacial shear rheology properties of asphaltene interfaces has generally been attributed to interactions and physical links between asphaltene molecules or aggregates[169, 171]. However, recently Samaniuk et al.[172] have shown that interfacial rheology data are consistent with a soft-glassy rheological behavior. This is a model for soft materials where rearrangements of species are difficult. The structural elements need to overcome an energy barrier to enter a new and more stable configuration. Consequently, the interfacial rheology properties would reflect a crowding of the interface[172].

Interfacial shear rheology has also been applied to understand the deposition of calcium naphthenate. This deposition is due to the presence of ARN tetrameric acids in oil[181]. This family of molecules has a very peculiar structure: fully aliphatic with a very high molecular weight (Mw≈1230 g/mol), it can be described as having 4 COOH function at the tips of 4 cycloalkyl arms[182]. It is present at the ppm level in oil but accumulated (tens of percents) in calcium naphtenate deposits[183]. The presence of ARN in oil is a prerequisite for the formation of calcium naphthenate deposition[184]. Interfacial shear rheology studies have shown that ARN tetrameric acid can react with Ca^{2+} at oil-water interface to form a gel if the pH is high enough to ionize ARN's carboxylic acid groups. The gel formation is strongly dependent on the crosslinking between ARN and Ca^{2+} and is thought to be the nucleation step of calcium naphthenate deposition. The gel strength is reduced in presence of calcium naphthenate inhibitors [175, 176, 177].

Recently, interfacial microrheology on asphaltene oil/water interface has been performed using a new ferromagnetic microbutton techniques. In addition to determining interfacial shear rheology moduli, this technique also allows to determine mechanical heterogeneities within the interface. Rheological heterogeneities of 10-100 μm in size can be detected [185].

3.2.2.3   Interfacial dilational rheology

Interfacial dilational rheology is measured using the sessile/pendant drop technique, also known as drop/bubble profile tensiometry (DPT) or axisymetrical drop shape analysis (ADSA). Here, a drop is formed at the tip of a capillary into a continuous phase (generally respectively oil and water for petroleum systems). This drop is illuminated and its profile is recorded with a camera. The profile depends of two forces

- Weight/buoyancy. This force is a function of the density difference between the drop phase and the continuous and tends to elongate the drop.
- The Young–Laplace equation. This tends to round the drop in a symmetrical way and depends on the drop radius and the interfacial tension.

If the densities of the two phases are known and after calibration of the droplet image (conversion of pixel to actual length), the software produces a series of theoretical profiles by changing the values of the interfacial tension. The curve that yields the best fit to the experimental points is then used to determine the measured interfacial tension[178].

The interfacial dilational properties of the drop interface are determined by varying the interfacial area while keeping the shape of interface nearly unaltered. Different variations are possible, but in most of the cases, the interfacial area A oscillates as:

$$\Delta A = A - A_0 = A_a \sin(\omega t) \tag{10}$$

A_α represents the amplitude area, A_0 is the equilibrium interfacial area, ΔA is the area change at any time t and ω is the angular frequency of oscillations.

The interfacial tension, measured with the method described above, also oscillates but with a phase shift. The complex dynamic apparent dilatational modulus (E^*) is then typically defined as the Fourier transform ($\mathcal{F}$) of the change in interfacial tension (γ) relative to the change in interfacial area via the following equation[186]:

$$E^*(\omega) = \frac{\mathcal{F}\{\Delta\gamma(t)\}}{\mathcal{F}\{\Delta\ln(A(t))\}} = E'(\omega) + iE''(\omega) \tag{11}$$

The complex modulus is split into a real and an imaginary part: the apparent elastic dilatational modulus E' and the apparent viscous dilatational modulus E''.

This technique presents pros and cons compared with interfacial shear rheology. Advantageously, the technique has less system limitations and it is generally easier to implement this method than interfacial shear rheology. The technique has also some drawbacks, i.e., if the bulk phase viscosity is too high, viscous forces can influence the shape of the drop during oscillation and affect the measured moduli. This influence can be quantified by a capillary number:

$$Ca = \frac{\Delta\eta \cdot \omega \cdot \Delta V}{\gamma \cdot a^2} \tag{12}$$

With Δη: difference of viscosity between the two bulk phases, ω: angular frequency of oscillations, Δ*V:* amplitude of volume oscillation, γ: equilibrium interfacial tension, *a*: radius of the capillary.

Viscous forces will influence the measured moduli if the Capillary number is beyond a given value[187]. Secondly, in some systems, the drop shape does not obey the Laplace equation which induces error in the calculation of interfacial tension when the interface is very rigid. For instance, in the case of adsorption of protein HFBII hydrophobin at air-water interface, the error of the Laplace equation fit of the drop profile strongly increases when the interface solidifies[188]. Mathematical treatments exist to consider extra stresses[189].

The interpretation of interfacial dilational rheology data is generally less straightforward than in the case of shear interfacial rheology. Schematically studies of asphaltenic interface by interfacial dilational rheology can be ranked into different categories:

- Bouriat et al.[190] have studied asphaltene solution in cyclohexane and diluted crude oil and asphaltene fractions at oil/water interface by performing frequency sweep at different temperatures and using the time/temperature super-imposition principle. This approach allows to determine the variations of E' and E'' on an extended range of frequency. Their results show that the asphaltene layer exhibits a glass transition zone and behaves as a gel near its gelation point.
- The Maxwell model, used to describe the viscoelastic properties of material, has been used to fit the variations of E' and E'' with frequency by Freer and Radke[191].
- Finally, Quintero et al.[192] have shown the applicability of the gelation theory (percolation) of Winter and Chambon[193] to describe the gelation kinetic at the interface between brine and a light crude oil.

Other studies consider adsorption to and desorption from the interface during the oscillatory variations of the interfacial area. These studies generally uses the Lucassen and van den Tempel (LVDT) model[194] to fit the variations of E' and E'' with bulk concentration. This model assumes that material transport is governed only by diffusion without energy barriers. This model allows to qualitatively explain that E' presents a maximum with bulk asphaltene concentration. However, a quantitative fit of the experimental data by the LVDT model requires that the asphaltene bulk diffusion coefficient decreases when the asphaltene concentration increases. Moreover, the calculated values of the diffusion coefficient are orders of magnitude lower than bulk values which raises questions concerning the validity of this approach[195, 196]

3.2.3   Small-Angle Neutron Scattering

Small-Angle Neutron Scattering (SANS) is a powerful technique to study the structure of colloidal system. SANS as well as its "sister" technique Small-Angle X-Ray Scattering (SAXS) has been extensively used to study the structure and the size and molecular weight of asphaltene aggregates[197] and ARN tetrameric acids[198]. However, to our knowledge, only 3 articles have been published using this technique to study interfaces in asphaltene-stabilized emulsions[199, 200, 201]. To our opinion, this lack of interest can be linked to the apparent complexity of the technique and the data analysis and, also, to the fact that SANS can only be performed in neutron facilities using research reactors or spallation sources to produce neutrons[202].

The scattering intensity I(q) of a colloid (volume v) in a solvent as a function of scattering vector q, defined as $4\pi\frac{\sin\theta}{\lambda}$ where 2θ is the deviation angle and λ the incident wavelength, is given by the following general expression[203]:

$$I(q) = \phi(1 - \phi)\Delta\rho^2 \cdot F(q) \cdot S(q) \qquad (13)$$

With ϕ: volume fraction; $\Delta\rho^2$: contrast factor; $F(q)$: the form factor normalised to the "scattering volume" v (i.e. F(0) = v), which is function of shape, size, and polydispersity of colloid; and $S(q)$: the structure factor which depends on the interparticle interactions.

The unique feature of this technique is the possibility to use isotope labelling to study specific parts. $\Delta\rho^2$ represents the contrast factor, i.e. ability of a system to scatter. The contrast factor represents the square difference between the scattering length density ρ of the solute and solvent. The scattering length density in SANS depends on the atomic composition of the solute or solvent and is equivalent to the refractive index in the case of light scattering and electron density for SAXS. The scattering length density of a compound is given by:

$$\rho = \frac{\rho_m \cdot N_A}{M} \sum_i n_i b_i \qquad (14)$$

With ρ_m: the mass density; M: the molecular weight; b_i: the scattering length of atom I; n_i: the number of atom de type I in the component; and N_A: the Avogadro Number. Tables give the neutron scattering length for the chemical elements and their isotopes. Consequently, the scattering length density of a component can be easily calculated if its composition and density are known. The scattering length of hydrogen and deuterium are very different (-0.374 vs. 0.667 10^{-12} cm)[204]. Consequently, by using deuterated solvent or mixture of hydrogenated solvent, the scattering density of the solvent can be adjusted to:

• Maximize the contrast factor to increase the signal and therefore decrease the analysis time. The incoherent scattering can also be reduced by using deuterated solvent which decreases the background.
• To see specific part of the solute if it is heterogeneous. For instance, if the solute consists in 2 parts with ρ_1 and ρ_2, the contrast between the solvent and the first part of the solute can be matched and are therefore "invisible" by SANS ($\rho_1 = \rho_{solvent}$) while allowing to specifically see and analyze the second part of the solute ($\rho_2 \neq \rho_{solvent}$).

Jestin et al.[200, 201] have developed a procedure to study model asphaltene-stabilized emulsions i.e. aqueous phase droplets dispersed in asphaltene solutions in xylene. After letting the droplets sediment, they transferred the dense-packed layers into a cuvette and analyzed them by SANS. They then use the possibility of contrast matching to observe specific part of the samples:

• By matching the scattering length density of the aqueous phase with the xylene phase's, only the signal from the asphaltene present at the interface is measured. The asphaltene layer thickness if then calculated by fitting the data with the form factor of a large flat disk.
• By equaling the scattering length density of asphaltenes and xylene solvent, the quantity of interface can be calculated (Porod's law). By independently measuring the concentrations of asphaltenes in the xylene phase before and after emulsification by UV-visible spectroscopy, the amount of asphaltenes at interface can be determined.

Verruto and Kilpatrick[199] have subsequently developed a different procedure to study similar model systems. The authors have fitted the SANS data with a planar sheet film and/or using a polydisperse core/shell form factor to determine the asphaltene film thickness the asphaltene volume fraction in the interfacial film. They have also deduced the film organic solvent and water content, and the amount of interface.

Fairly similar conclusions are obtained from the two methods when applied on model systems (solvents: xylene for Jestin et al.; toluene, 1-methylnaphthalene, and decalin for Verruto and Kilpatrick): Adsorbed amount at interface (xylene only) ≈ 2 mg/m^2, volume fraction of asphaltenes in adsorbed layer $\approx 10 - 30$ %, and thickness adsorbed layer of 10-15 nanometers. Measured parameters varied with the pH of the aqueous phase, the polarity of the oil phase, the presence of resins, and the ageing.

3.3 Oil-water separation assessment at the laboratory scale

Water is co-produced with crude oil and form water-in-oil emulsions. These emulsions need to be resolved to be able to produce anhydrous oil and water free of oil that could be discharged or reinjected into the formation. Quantitatively, the maximum water content in oil must be lower than 0.5 wt %. The regulation concerning produced water quality depends on countries. For instance in USA, the permitted monthly average and daily maximum concentrations of total oil and grease are 29 and 42 mg/L[205].

Oil-water separation is usually performed in 2-3 gravity separators placed in series. The separation is based on the sedimentation, flocculation and coalescence of droplets. Demulsification is sped up with the addition of chemical demulsifiers and, in some facilities, presence of electrocoalescers. Produced water is collected from the gravity separators and pass through other purification steps to meet the regulation. These steps can involve skimmers, hydrocyclones, flotation units, membrane filtration and so on[206, 207] to meet the final level of contamination of the produced water. This level is 30 ppm in Norway.

A current trend in offshore crude oil production is to perform a part of the required separation process at the seabed instead of in the platform to save energy. Subsea separation and disposal of the produced water for instance by directing it back to the seafloor for re-injection, allows to avoid the transportation of unwanted components to the platform as well as reduce the size of the topside process and the flowlines and risers[208]. However, the designed subsea separation process should be very robust and require little maintenance since intervention would be costly. In addition, future process modification would not be, or with difficulty, possible.

In order to design an efficient separation strategy, the oil-water separation needs to be evaluated at the laboratory scale. The techniques used in this evaluation can be combined with techniques presented in section 3.2 to be able to understand and predict the crude oil emulsion stability.

The traditional technique to evaluate emulsion stability consists of preparing emulsions in batch at volumes $\approx$ 10-100 mL and then follow-up the appearance of free water with time (bottle tests). New techniques and procedures such as NMR have been introduced to increase the quantity and quality of information obtained during batch separation (section 3.3.1.2). Recently, microfluidic techniques have been introduced to study droplet coalescence (section 3.3.2).

3.3.1 Emulsion preparation and evaluation

3.3.1.1 Emulsion preparation

The first part in studying emulsion stability at laboratory conditions is to prepare water-in-oil emulsions and test corresponding stability under preparation conditions separation and transport under real process conditions. Several points must be considered.

Crude oil sampling is critical. They should not be contaminated by production chemicals like drilling mud, corrosion inhibitor, or demulsifier. The presence of these additives would completely change the separation kinetic of crude oil emulsion. Crude oil can also be pressurized (live oil). Analysis of live oils require specific and costly devices, but test conditions are of course closer to real ones due to the presence of a gas component[209]. Dead samples are much easier to handle and analyze but they can be oxidized in atmosphere[210].

Most of the study are performed at atmospheric pressure using dead oils. Emulsions are prepared by mixing crude oil and brine using devices such as propellers or rotor-stator homogenizers like Ultra-Turrax. The high shearing will break up droplets into smaller droplets.

The average droplet diameter and the droplet size diameter (DSD) distribution determined right after emulsification is an important parameter to determine since they condition the separation kinetic. Indeed, bigger droplets sediment faster than smaller ones. DSD represents the droplet amount according to their size. The DSD is the bridge between laboratory and real conditions.

The prediction of the droplet size diameter as a function of the emulsification conditions and fluid characteristics is complex and reviews exist[211, 212, 213]. Some basic concepts are presented here.

The droplet diameter depends primally of the flow regime, which is characterized by the Reynolds number Re:

$$Re = \frac{L \cdot \bar{v} \cdot \rho_C}{\eta_C} \qquad (15)$$

With L: a characteristic length of the system; $\bar{v}$: the average fluid velocity; ρ_C and η_C: are respectively the density and the viscosity of the fluid. Two Reynolds number can be defined, one for the continuous phase (Re[fluid]), one for the droplet (Re[droplet]). In the latter, the characteristic length is the droplet diameter. Below a critical Reynolds number, the flow is laminar, and turbulent above.

A starting case is the droplet break-up in laminar flow. In this case Re[fluid]<~1000 and Re[droplet]<1. This case was analyzed by Grace[214]. A stress is exerted on a droplet due to the flow and is counteracted by the Laplace pressure. The ratio of these two phenomena is given by the Weber number We:

$$We = \frac{\eta_C \cdot G \cdot r}{\gamma} \qquad (16)$$

With η_C: the viscosity of the continuous phase, G: the shear rate, r: the droplet radius, and γ: the interfacial tension. The droplet bursts into smaller ones if the Weber number is higher than a critical value We_{cr}. This critical value depends on the ratio of the viscosity of dispersed phase η_D to the continuous phase one (Figure 8). This figure shows that the smallest droplets are created when the viscosity of the dispersed phase is slightly lower than the viscosity of the dispersed phase. If the viscosity of the two phases are very different, higher shear rate must be applied to break up the droplets. The following equation allows to estimate the maximum droplet diameter d_max after homogeneization under steady-state conditions[213]:

$$d_{max} = \frac{2 \cdot \gamma \cdot We_C}{G \cdot \eta_C} \qquad (17)$$
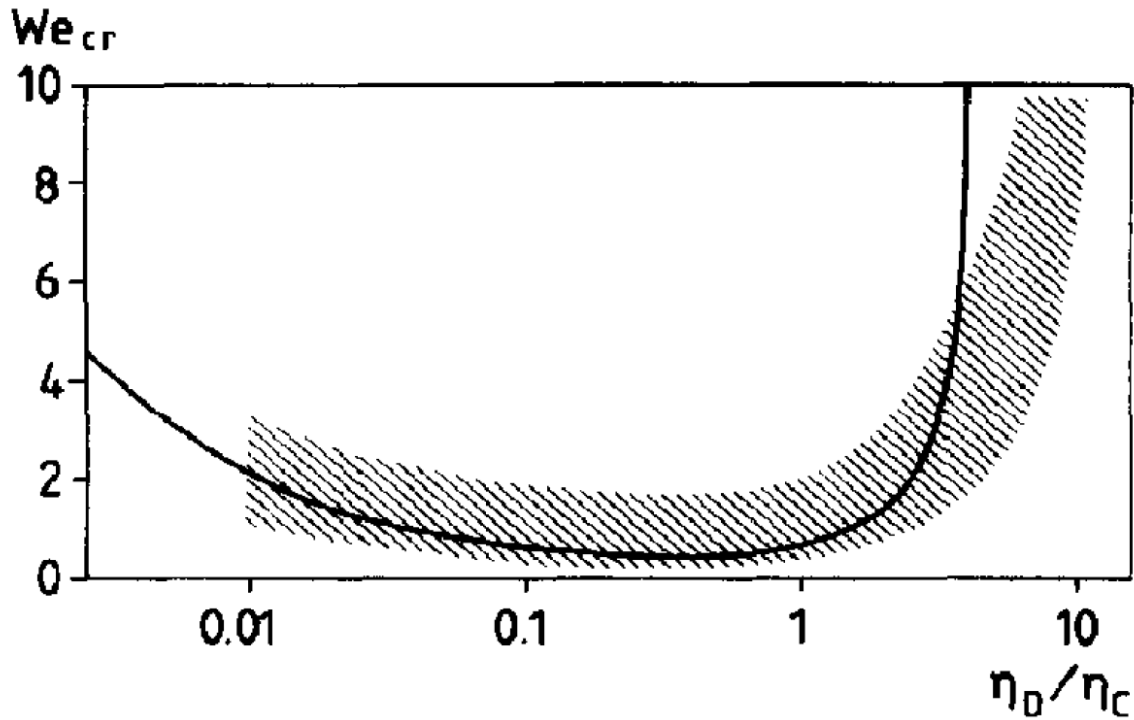
Figure 8: Effect of viscosity ratio on the critical Weber number characterizing the droplet breakup in shear flow. The curve are results by Grace[214] and the hatched area are average droplet sizes in a colloid mill by Ambruster. Figure by Walstra[211]. Reprinted with permission. Copyright 1993 Elsevier.

The turbulent flow is characterized by the presence of eddies. Two regimes have to be considered[212, 213]:

•   The regime is Turbulent-viscous (Re[fluid]>~2000 and Re[droplet]<1). In this case the maximum droplet diameter during homogenization under steady-state conditions is given by:

$$d_{max} = \frac{\gamma}{(\varepsilon \cdot \eta_C)^{1/2}} \qquad (18)$$

With ε: the energy, i.e. the energy dissipated by time unit and volume unit.

•   The regime is Turbulent-inertial (Re[fluid]>~2000 and Re[droplet]>1). The maximum droplet diameter is:

$$d_{max} = \left(\frac{\gamma^3}{\varepsilon^2 \cdot \rho_C}\right)^{1/5} \qquad (19)$$

Different methods exist to determine DSD and average droplet diameter: video microscopy[215, 216, 217, 218], diffraction method using the Malvern "Mastersizer" or any equivalent apparatus, counter coulter apparatus (only valid for o/w emulsions). However, these techniques often require dilution of the sample which can influence the final results. The emulsions are generally diluted with the dispersing phase including surfactant stabilizing emulsions to minimize desorption of stabilizing species from

interface and coalescence. In addition, in the case of microscopy, the smallest droplets can be difficult to distinguish from the background.

NMR procedures allow to determine DSD with no dilution. These techniques are presented in section 3.3.1.2.

3.3.1.2   Crude oil emulsion stability evaluation

Crude oil emulsion stability is evaluated by classical bottle testing. After emulsification and possible addition of demulsifiers, emulsions are transferred in graduated flask. The kinetic of free water appearance is then reported by visually logging the volume of free water as a function of time. The residual water content in the top phase can be determined at the end of the test by taking a small aliquot at the top of the sample and measure the water content by Karl Fischer Titration [219] or by NMR.

This method is still widely used. However, devices have been developed that allow to automatize the measurements or obtain more parameters to characterize and follow the separation.

Turbiscan measures the transmitted and back scattered light intensity with the height of the sample and has been implemented to follow-up the water separation in w/o [220, 221] and o/w emulsions[218]. Van Dick et al. have used conductivity measurements to follow up demulsification of crude oil emulsions[222]. Hurtevent et al. [223] have followed up the oil-water separation using a an ultra-sound transducers to measure oil/water fraction as a function of the height and time. They were able to measure the position of different interfaces (sedimentation interface, dense-packed zone, coalescence interface) with time.

At the industrial scale, different sensor technologies exist to monitor the position of the interfaces as reviewed by Bukhari et Yang [224]. Their classification is the following:

- Externally mounted displacers. A displacer is present at the interface and its position is monitored as it moves up and down.
- Differential pressure transmitters: the pressure difference between the oil and water phases is measured.
- Ultrasonic transducers: The ultrasonic signal of an emitter is received and analyzed by a receiver.
- Gamma ray sensors. A source emits low energy gamma-ray that is detected and analyzed.
- Multi-electrode capacitance level sensors which are composed of an array of capacitance electrodes installed vertically[225].

Recent development in techniques to follow oil-water separation at the bench scale involves ^{1}H Nuclear Magnetic Resonance. This method has been applied to study crude oil emulsions but until a few years ago some restrictions limited its implementation:

-The shape of the droplet size distribution (DSD) was assumed when measuring it[226, 227].

-The measurement time was sometimes excessive to follow-up a separation[228].

Recently, new ^{1}H NMR procedures have been developed that do not require assumptions and allows to determine DSD and profiles in the minute timescale. These procedures allow:

-To determine the droplet size distribution of the sample. The shape of the DSD is determined by measuring the distribution of T_2 relaxation times while the absolute diameter values are determined by following the restricted diffusion of water molecules inside the droplets[229].

-To measure the brine profile i.e. the brine content at different heights of the sample. Measuring the brine content at different times allows to determine isoprofile curves, that means variations of the position of a specific brine content as a function of times. This makes it possible to determine the variation of the free water content with time as well as the droplet sedimentation rate[230].

-NMR can also be used to determine the residual water content at the top of the oil phase[231].

The NMR procedures have been developed on a 23 MHz machine. This low-field NMR bench scale uses a permanent magnet[232] and are cheaper and easier to handle than traditional high field (600 MHz for instance) NMR spectrometer that uses liquid helium and nitrogen to cool-down the superconducting magnet.

The procedures presented above requires to analyze the data of the brine phase only. As low-field NMR apparatus do not allow to use chemical shifts to separate oil and brine contributions to the oil signal, other methods need to be implemented. According to Sørland[232], these methods are based on " relaxation times, the difference in temperature dependency on the viscosity, the mobility, or the observation time dependency on the root of the mean squared displacement" of the oil and brine phases.

The NMR procedures have been implemented to study the demulsification of water-in-crude oil emulsions by chemical demulsifiers[233]. Data obtained by NMR have been compared with predictions from a population balance model [234].

3.3.2   Microfluidic techniques

Microfluidic is the science that controls and handles flow in channels where one dimension is in the order of micrometers[235]. That means that small amounts of fluids (10^{-9} to 10^{-18} liters) are handled in a typical experiment. Microfluid has found many applications in various fields in the last 20-30 years such as in analytical chemistry, biology (DNA and enzyme analysis, immunoassays, cytometry, biosensors, culturing)[236], and engineering (printing devices).

One of the sub-categories of microfluidic is droplet-based microfluid. It focuses on the creation of discrete volumes with the use of immiscible phases[237]. Droplet microfluidic can be used to study flocculation and coalescence of droplets under flow. A typical setup is presented in Figure 9 [238]. This setup comprises:

- 2 Pumps, one for each of the phase.
- Droplets are created as a result of the shear stress exerted by the flow of the carrier fluid using a special geometry. The figure presents a perpendicular T-junction that creates a cross flow. Two other geometries are possible: flow focusing and co-flow. Droplets formed are monodisperse.
- The droplets enter a channel where they collide and coalesce. Here a high-speed camera records flocculation of coalescence phenomena.
- The movies recorded are analyzed to quantify, for instance, the coalescence frequency.
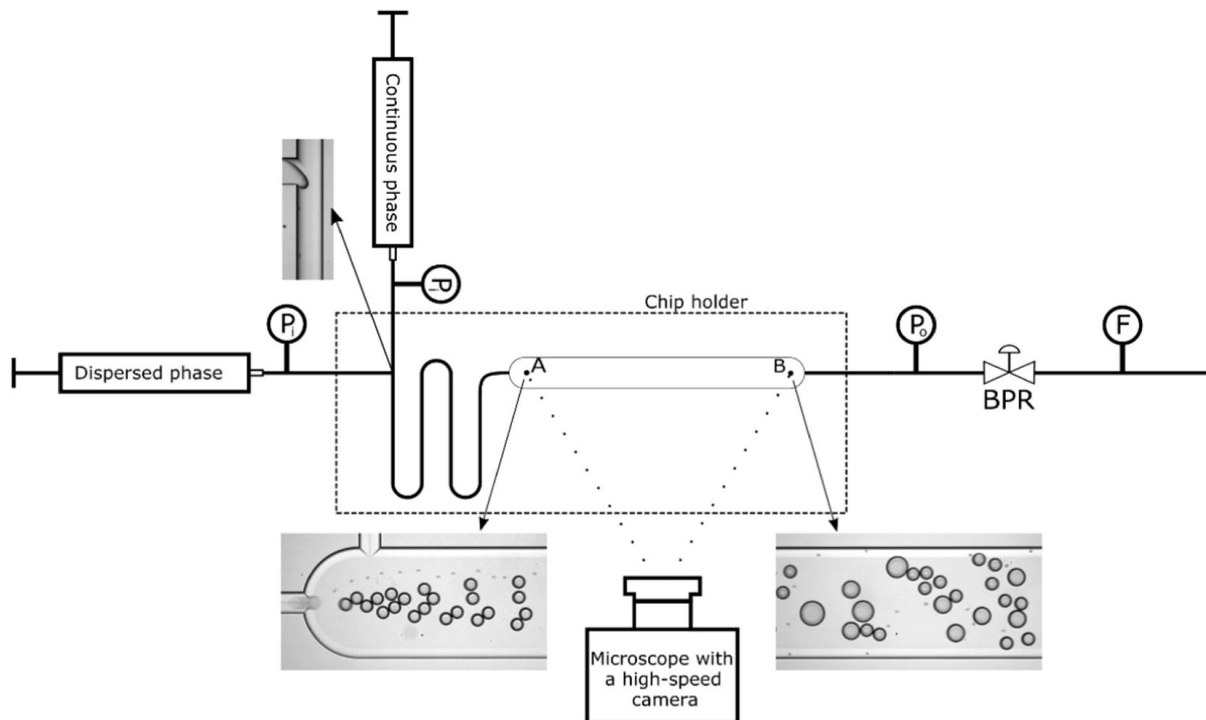
Figure 9: Scheme of a microfluidic setup and chips. BPR: backpressure regulator; P: pressure sensor; F: flowmeter. Scheme by Dudek et al.[238]. Reprinted with permission. Copyright 2018 Elsevier.

Several advantages make this technique advantageous to study emulsions[239].

- The formed droplets have a narrow DSD.
- The droplet diameter can be controlled by adjusting flow rates.
- Possibility to visualize coalescence or flocculation phenomena.
- Emulsions are studied under flow conditions.
- The sample volume is small.
- High heat and mass transfer rates.
- Decreased analysis time and increased reproducibility.
- Possibility of measurements under high pressure and high temperature.

Numerous studies have focused on the study of petroleum emulsions and emphasizing the possible applications of microfluidic:

Dudek et al. have studied the coalescence of diluted crude oil in water emulsions to understand produced water separation. They have compared the coalescence frequency of these systems by varying the origin of the crude oil, the pH of the aqueous phase, the presence of dissolved components in the aqueous phase and the pressure[238, 240]. The same authors have subsequently studied the attachment of crude oil droplets to gas bubbles to understand phenomena in flotation units used in produced water treatment. The setup presented in Figure 9 was modified to incorporate an extra T-junction to generate gas bubbles. From image analysis, they determined the attachment efficiency between bubbles and droplets to study the influence of various parameters[241].

Lin et al.[242] have applied microfluidic to study asphaltenes-Stabilized water-in-oil (w/o) emulsions. The oil phase was composed of asphaltenes in a mixture of heptane and toluene. They measured the droplet coalescence rate in presence of surfactant or microemulsion with and without demulsifiers. Nowbahar et al.[243] have studied the coalescence of water droplets in diluted bitumen to understand the Clark Hot Water Extraction process used in bitumen production. Their microfluidic device was composed of a long serpentine channel which allows to observe droplets for a time sufficient to determine the number of coalescence events as a function of the residence time in the channel. The kinetics of coalescence of water droplets were measured in presence of different chemical additives. They also visually assessed the presence of flocculation.

In microfluidic, droplets are confined and sometimes squeezed between the top and the bottom walls of the channels. The confinement influences coalescence and droplet breakup. Chen et al.[244] have found that confinement promotes coalescence of unperturbated droplets in sheared flow using a counter rotating shear flow device. Using the same device, Vananroye et al.[245] have studied the effect of droplet confinement on the droplet breakup in sheared flow. They found that for low viscosity ratios between the dispersed phase and the dispersing phase, confinement suppresses breakup, whereas for high viscosity ratios, confinement promotes breakup. These results indicate that the timescale of studied events obtained by microfluidic may differ from real processes[239].

4   Concluding remarks

A large selection of experimental techniques exist to characterize complex crude oil systems to mitigate flow assurance and separation issues. Two specific issues have been considered in the review: Wax deposition and gelation as well as stabilization of crude oil emulsions by asphaltenes.

Waxes can cause production irregularities through wax crystallization, waxy gelling and wax deposition, which is predominantly driven by temperature gradients during pipeline transport. Assessing the onset and severity of wax crystallization is therefore important to design and evaluate counter measures. The total amount of waxes in crude oil can be measured by several techniques (e.g. acetone precipitation method, DSC, FTIR, ^{1}H NMR) while their composition can be determined by gas chromatography. The wax appearance temperature (WAT) is an important parameter that will indicate the temperature at which waxes start precipitating and production issues start appearing. Several methods can be implemented to measure WAT, traditionally employing techniques such as cross-polarized microscopy (CPM), rheometry and differential scanning calorimetry (DSC). Recent progress extends the scope of techniques to near-infrared scattering (NIR) or nuclear magnetic resonance (NMR), but also improve procedures for established techniques, e.g. via modulated DSC or dynamic rheology measurements. However, the obtained values depend on the measurement technique as well as experimental parameters, primarily the cooling rate, and therefore the obtained data must be interpreted with care. Different techniques and experimental procedures have been developed to characterize the main issues of waxes: Viscosity increase and gelation, pipeline start-in, and deposition. The first issues are generally characterized at bench scale by rheology, for which multiple protocols are described in the literature. Deposition can be assessed using the cold finger apparatus at bench scale and flow loops at industrial scale. Finally, multiple techniques and sample preparation procedures are available to study the wax crystallization mechanism as well as the influence of crude oil components and wax inhibitor on it.

Asphaltenes are a complex mixture, for which a part of the composition can be determined by FT-ICR MS. New fractionation techniques based on adsorption on polar surfaces (water or hydrophilic solid) have been developed to obtain fractions of reduced complexity allowing to find out correlation between chemical functionalities and crude oil properties. The structure and properties of the asphaltene layer formed at the interface between water droplets and the oil continuous phase can now be described. The thickness of the layer, its solvation degree as well as adsorbed amount can de deduced from IFT and SANS measurements. Progress in the instrumentation allows to measure both the shear and dilational rheological properties of the asphaltene interface. Several models have been proposed to interpret the interfacial rheology data and a synthesis of the results is necessary. Finally, new techniques are also available to study the stability of crude oil emulsions and oil-water separation. Droplet microfluidic allows to visually observe and quantify the coalescence between droplets. At larger scales, NMR techniques allows to follow-up oil-water separation by measuring the brine profile with the height of sample as well the droplet size distribution.

5   Acknowledgement

6   References

1.   Sjöblom, J.; Aske, N.; Harald Auflem, I.; Brandal, O.; Erik Havre, T.; Saether, O.; Westvik, A.; Eng Johnsen, E.; Kallevik, H. Our Current Understanding of Water-in-Crude Oil Emulsions.: Recent Characterization Techniques and High Pressure Performance. *Adv. Colloid Interface Sci.* **2003,** *100-102*, 399-473.
2.   Aske, N.; Kallevik, H.; Sjöblom, J. Determination of Saturate, Aromatic, Resin, and Asphaltenic (SARA) Components in Crude Oils by Means of Infrared and Near-Infrared Spectroscopy. *Energy & Fuels* **2001,** *15* (5), 1304-1312.
3.   Hannisdal, A.; Hemmingsen, P. V.; Sjoblom, J. Group-Type Analysis of Heavy Crude Oils Using Vibrational Spectroscopy in Combination with Multivariate Analysis. *Industrial & Engineering Chemistry Research* **2005,** *44* (5), 1349-1357.
4.   Suatoni, J. C.; Swab, R. E. Rapid hydrocarbon group-type analysis by high performance liquid chromatography. *Journal of Chromatographic Science* **1975,** *13* (8), 361-366.

5.   Lundanes, E.; Greibrokk, T. Separation of fuels, heavy fractions, and crude oils into compound classes: A review. *Journal of High Resolution Chromatography* **1994,** *17* (4), 197-202.

6.   Hemmingsen, P. V.; Kim, S.; Pettersen, H. E.; Rodgers, R. P.; Sjoblom, J.; Marshall, A. G. Structural Characterization and Interfacial Behavior of Acidic Compounds Extracted from a North Sea Oil. *Energy Fuels* **2006,** *20* (5), 1980-1987.

7.   Qian, K.; Rodgers, R. P.; Hendrickson, C. L.; Emmett, M. R.; Marshall, A. G. Reading Chemical Fine Print: Resolution and Identification of 3000 Nitrogen-Containing Aromatic Compounds from a Single Electrospray Ionization Fourier Transform Ion Cyclotron Resonance Mass Spectrum of Heavy Petroleum Crude Oil. *Energy & Fuels* **2001,** *15* (2), 492-498.

8.   Mapolelo, M. M.; Rodgers, R. P.; Blakney, G. T.; Yen, A. T.; Asomaning, S.; Marshall, A. G. Characterization of naphthenic acids in crude oils and naphthenates by electrospray ionization FT-ICR mass spectrometry. *Int. J. Mass Spectrom.* **2011,** *300* (2–3), 149-157.

9.   Brandal, O.; Hanneseth, A.-M. D.; Hemmingsen, P. V.; Sjoblom, J.; Kim, S.; Rodgers, R. P.; Marshall, A. G. Isolation and Characterization of Naphthenic Acids from a Metal Naphthenate Deposit: Molecular Properties at Oil-Water and Air-Water Interfaces. *J. Dispersion Sci. Technol.* **2006,** *27* (3), 295 - 305.

10.   Qian, K.; Robbins, W. K.; Hughey, C. A.; Cooper, H. J.; Rodgers, R. P.; Marshall, A. G. Resolution and Identification of Elemental Compositions for More than 3000 Crude Acids in Heavy Petroleum by Negative-Ion Microelectrospray High-Field Fourier Transform Ion Cyclotron Resonance Mass Spectrometry. *Energy Fuels* **2001,** *15* (6), 1505-1511.

11.   Marshall, A. G.; Rodgers, R. P. Petroleomics: The Next Grand Challenge for Chemical Analysis. *Accounts of Chemical Research* **2004,** *37* (1), 53-59.

12.   Rodgers, R. P.; Schaub, T. M.; Marshall, A. G. Petroleomics: MS Returns to Its Roots. *Analytical chemistry* **2005,** *77* (1), 20 A-27 A.

13.   Kim, S.; Kramer, R. W.; Hatcher, P. G. Graphical Method for Analysis of Ultrahigh-Resolution Broadband Mass Spectra of Natural Organic Matter, the Van Krevelen Diagram. *Analytical Chemistry* **2003,** *75* (20), 5336-5344.

14.   Pereira, T. M. C.; Vanini, G.; Tose, L. V.; Cardoso, F. M. R.; Fleming, F. P.; Rosa, P. T. V.; Thompson, C. J.; Castro, E. V. R.; Vaz, B. G.; Romão, W. FT-ICR MS analysis of asphaltenes: Asphaltenes go in, fullerenes come out. *Fuel* **2014,** *131*, 49-58.

15.   Pereira, T. M. C.; Vanini, G.; Oliveira, E. C. S.; Cardoso, F. M. R.; Fleming, F. P.; Neto, A. C.; Lacerda Jr, V.; Castro, E. V. R.; Vaz, B. G.; Romão, W. An evaluation of the aromaticity of asphaltenes using atmospheric pressure photoionization Fourier transform ion cyclotron resonance mass spectrometry – APPI(±)FT-ICR MS. *Fuel* **2014,** *118*, 348-357.

16.   Nascimento, P. T. H.; Santos, A. F.; Yamamoto, C. I.; Tose, L. V.; Barros, E. V.; Gonçalves, G. R.; Freitas, J. C. C.; Vaz, B. G.; Romão, W.; Scheer, A. P. Fractionation of Asphaltene by Adsorption onto Silica and Chemical Characterization by Atmospheric Pressure Photoionization Fourier Transform Ion Cyclotron Resonance Mass Spectrometry, Fourier Transform Infrared Spectroscopy Coupled to Attenuated Total Reflectance, and Proton Nuclear Magnetic Resonance. *Energy & Fuels* **2016,** *30* (7), 5439-5448.

17.   Chacón-Patiño, M. L.; Rowland, S. M.; Rodgers, R. P. Advances in Asphaltene Petroleomics. Part 1: Asphaltenes Are Composed of Abundant Island and Archipelago Structural Motifs. *Energy & Fuels* **2017,** *31* (12), 13509-13518.

18.   Rowland, S. M.; Robbins, W. K.; Corilo, Y. E.; Marshall, A. G.; Rodgers, R. P. Solid-Phase Extraction Fractionation To Extend the Characterization of Naphthenic Acids in Crude Oil by Electrospray Ionization Fourier Transform Ion Cyclotron Resonance Mass Spectrometry. *Energy & Fuels* **2014,** *28* (8), 5043-5048.

19.   Mullins, O. C. Petroleomics and Structure Function Relations in Asphaltenes and Crude Oils. In *Asphaltenes, Heavy Oils, and Petroleomics*, O.C. Mullins, E. Y. S., A. Hammami, A.G. Marshall, Ed.; Springer: New York, 2007, pp 1-16.

20.   Yang, F.; Zhao, Y.; Sjöblom, J.; Li, C.; Paso, K. G. Polymeric Wax Inhibitors and Pour Point Depressants for Waxy Crude Oils: A Critical Review. *Journal of Dispersion Science and Technology* **2015,** *36* (2), 213-225.

21.   Kelland, M. A. *Production chemicals for the oil and gas industry*; second ed.; CRC press: Boca Raton, 2014.

22.   Roenningsen, H. P.; Bjoerndal, B.; Baltzer Hansen, A.; Batsberg Pedersen, W. Wax precipitation from North Sea crude oils: 1. Crystallization and dissolution temperatures, and Newtonian and non-Newtonian flow properties. *Energy & Fuels* **1991,** *5* (6), 895-908.

23.   Kurniawan, M.; Subramanian, S.; Norrman, J.; Paso, K. Influence of Microcrystalline Wax on the Properties of Model Wax-Oil Gels. *Energy & Fuels* **2018,** *32* (5), 5857-5867.

24.   Burger, E. D.; Perkins, T. K.; Striegler, J. H. Studies of Wax Deposition in the Trans Alaska Pipeline. *Journal of Petroleum Technology* **1981,** *33* (06), 1075-1086.

25.   Chen, J.; Zhang, J.; Li, H. Determining the wax content of crude oils by using differential scanning calorimetry. *Thermochimica Acta* **2004,** *410* (1–2), 23-26.

26.   Monger-McClure, T. G.; Tackett, J. E.; Merrill, L. S. Comparisons of Cloud Point Measurement and Paraffin Prediction Methods. **1999.**

27.   von Mühlen, C.; de Oliveira, E. C.; Zini, C. A.; Caramão, E. B.; Marriott, P. J. Characterization of Nitrogen-Containing Compounds in Heavy Gas Oil Petroleum Fractions Using Comprehensive Two-Dimensional Gas Chromatography Coupled to Time-of-Flight Mass Spectrometry. *Energy & Fuels* **2010,** *24* (6), 3572-3580.

28.   Batsberg Pedersen, W.; Baltzer Hansen, A.; Larsen, E.; Nielsen, A. B.; Roenningsen, H. P. Wax precipitation from North Sea crude oils. 2. Solid-phase content as function of temperature determined by pulsed NMR. *Energy & fuels* **1991,** *5* (6), 908-913.

29.   Zhao, Y.; Paso, K.; Norrman, J.; Ali, H.; Sørland, G.; Sjöblom, J. Utilization of DSC, NIR, and NMR for wax appearance temperature and chemical additive performance characterization. *J Therm Anal Calorim* **2015,** *120* (2), 1427-1433.

30.   Saxena, H.; Majhi, A.; Behera, B. Prediction of wax content in crude oil and petroleum fraction by proton NMR. *Petroleum Science and Technology* **2019,** *37* (2), 226-233.

31.   Coto, B.; Martos, C.; Espada, J. J.; Robustillo, M. D.; Peña, J. L. Analysis of paraffin precipitation from petroleum mixtures by means of DSC: Iterative procedure considering solid–liquid equilibrium equations. *Fuel* **2010,** *89* (5), 1087-1094.

32.   Roehner, R. M.; Hanson, F. V. Determination of Wax Precipitation Temperature and Amount of Precipitated Solid Wax versus Temperature for Crude Oils Using FT-IR Spectroscopy. *Energy & Fuels* **2001,** *15* (3), 756-763.

33.   Robustillo, M. D.; Coto, B.; Martos, C.; Espada, J. J. Assessment of Different Methods To Determine the Total Wax Content of Crude Oils. *Energy & Fuels* **2012,** *26* (10), 6352-6357.

34.   Speight, J. G. Petroleum Asphaltenes - Part 1: Asphaltenes, Resins and the Structure of Petroleum *Oil & Gas Science and Technology* **2004,** *59* (5), 467-477

35.   Murgich, J. Molecular Simulation and the Aggregation of the Heavy Fractions in Crude Oils. *Molecular Simulation* **2003,** *29* (6-7), 451-461.

36.   Mitra-Kirtley, S.; Mullins, O. C.; Ralston, C. Y.; Sellis, D.; Pareis, C. Determination of Sulfur Species in Asphaltene, Resin, and Oil Fractions of Crude Oils. *Appl. Spectrosc.* **1998,** *52* (12), 1522-1525.

37.   Mitra-Kirtley, S.; Mullins, O. C.; Van Elp, J.; George, S. J.; Chen, J.; Cramer, S. P. Determination of the nitrogen chemical structures in petroleum asphaltenes using XANES spectroscopy. *Journal of the American Chemical Society* **1993,** *115* (1), 252-258.

38.   Friberg, S. E. Micellization. In *Asphaltenes, Heavy Oils, and Petroleomics*, Mullins, O. C.; Sheu, E. Y.; Hammani, A.; Marshall, A. G., Eds.; Springer Science+Business Media: New York, 2007, pp 189-203.

39.	Jian, C.; Tang, T.; Bhattacharjee, S. Probing the Effect of Side-Chain Length on the Aggregation of a Model Asphaltene Using Molecular Dynamics Simulations. *Energy & Fuels* **2013,** *27* (4), 2057-2067.

40.	Subramanian, S.; Simon, S.; Sjöblom, J. Interaction between asphaltenes and fatty-alkylamine inhibitor in bulk solution. *Journal of Dispersion Science and Technology* **2018,** *39* (2), 163-173.

41.	Teklebrhan, R. B.; Ge, L.; Bhattacharjee, S.; Xu, Z.; Sjöblom, J. Probing Structure–Nanoaggregation Relations of Polyaromatic Surfactants: A Molecular Dynamics Simulation and Dynamic Light Scattering Study. *The Journal of Physical Chemistry B* **2012,** *116* (20), 5907-5918.

42.	Sjöblom, J.; Simon, S.; Xu, Z. Model molecules mimicking asphaltenes. *Advances in Colloid and Interface Science* **2015,** *218* (0), 1-16.

43.	Akbarzadeh, K.; Bressler, D. C.; Wang, J.; Gawrys, K. L.; Gray, M. R.; Kilpatrick, P. K.; Yarranton, H. W. Association Behavior of Pyrene Compounds as Models for Asphaltenes. *Energy Fuels* **2005,** *19* (4), 1268-1271.

44.	Tan, X.; Fenniri, H.; Gray, M. R. Pyrene Derivatives of 2,2'-Bipyridine as Models for Asphaltenes: Synthesis, Characterization, and Supramolecular Organization. *Energy & Fuels* **2007,** *22* (2), 715-720.

45.	Rakotondradany, F.; Fenniri, H.; Rahimi, P.; Gawrys, K. L.; Kilpatrick, P. K.; Gray, M. R. Hexabenzocoronene Model Compounds for Asphaltene Fractions: Synthesis & Characterization. *Energy Fuels* **2006,** *20* (6), 2439-2447.

46.	Alshareef, A. H.; Scherer, A.; Stryker, J. M.; Tykwinski, R. R.; Gray, M. R. Thermal Cracking of Substituted Cholestane–Benzoquinoline Asphaltene Model Compounds. *Energy & Fuels* **2012,** *26* (6), 3592-3603.

47.	Nordgård, E. L.; Sjöblom, J. Model Compounds for Asphaltenes and C80 Isoprenoid Tetraacids. Part I: Synthesis and Interfacial Activities. *J. Dispersion Sci. Technol.* **2008,** *29* (8), 1114 -1122.

48.	Alshareef, A. H.; Scherer, A.; Tan, X.; Azyat, K.; Stryker, J. M.; Tykwinski, R. R.; Gray, M. R. Effect of Chemical Structure on the Cracking and Coking of Archipelago Model Compounds Representative of Asphaltenes. *Energy & Fuels* **2012,** *26* (3), 1828-1843.

49.	Nordgård, E. L.; Landsem, E.; Sjöblom, J. Langmuir Films of Asphaltene Model Compounds and Their Fluorescent Properties. *Langmuir* **2008,** *24* (16), 8742-8751.

50.	Nordgård, E. L.; Sørland, G.; Sjöblom, J. Behavior of Asphaltene Model Compounds at W/O Interfaces. *Langmuir* **2009,** *26* (4), 2352-2360.

51.	Pradilla, D.; Simon, S.; Sjöblom, J.; Samaniuk, J.; Piechochka, M.; Vermant, J. Sorption and Interfacial Rheology Study of Model Asphaltene Compounds. *To be submitted to Langmuir* **2016**.

52.	Pradilla, D.; Subramanian, S.; Simon, S.; Sjöblom, J.; Beurroies, I.; Denoyel, R. Microcalorimetry Study of the Adsorption of Asphaltenes and Asphaltene Model Compounds at the Liquid–Solid Surface. *Langmuir* **2016,** *32* (29), 7294-7305.

53.	Kuznicki, T.; Masliyah, J. H.; Bhattacharjee, S. Aggregation and Partitioning of Model Asphaltenes at Toluene–Water Interfaces: Molecular Dynamics Simulations. *Energy & Fuels* **2009,** *23* (10), 5027-5035.

54.	Fossen, M.; Kallevik, H.; Knudsen, K. D.; Sjöblom, J. Asphaltenes Precipitated by a Two-Step Precipitation Procedure. 1. Interfacial Tension and Solvent Properties. *Energy & Fuels* **2007,** *21* (2), 1030-1037.

55.	Spiecker, P. M.; Gawrys, K. L.; Kilpatrick, P. K. Aggregation and solubility behavior of asphaltenes and their subfractions. *Journal of Colloid and Interface Science* **2003,** *267* (1), 178-193.

56.	Qiao, P.; Harbottle, D.; Tchoukov, P.; Masliyah, J.; Sjoblom, J.; Liu, Q.; Xu, Z. Fractionation of Asphaltenes in Understanding Their Role in Petroleum Emulsion Stability and Fouling. *Energy & Fuels* **2017,** *31* (4), 3330-3337.

57.   Yang, F.; Tchoukov, P.; Pensini, E.; Dabros, T.; Czarnecki, J.; Masliyah, J.; Xu, Z. Asphaltene Subfractions Responsible for Stabilizing Water-in-Crude Oil Emulsions. Part 1: Interfacial Behaviors. *Energy & Fuels* **2014,** *28* (11), 6897-6904.

58.   Yang, F.; Tchoukov, P.; Dettman, H.; Teklebrhan, R. B.; Liu, L.; Dabros, T.; Czarnecki, J.; Masliyah, J.; Xu, Z. Asphaltene Subfractions Responsible for Stabilizing Water-in-Crude Oil Emulsions. Part 2: Molecular Representations and Molecular Dynamics Simulations. *Energy & Fuels* **2015,** *29* (8), 4783-4794.

59.   Subramanian, S.; Simon, S.; Gao, B.; Sjöblom, J. Asphaltene fractionation based on adsorption onto calcium carbonate: Part 1. Characterization of sub-fractions and QCM-D measurements. *Colloids and Surfaces A: Physicochemical and Engineering Aspects* **2016,** *495*, 136-148.

60.   Subramanian, S.; Sørland, G. H.; Simon, S.; Xu, Z.; Sjöblom, J. Asphaltene fractionation based on adsorption onto calcium carbonate: Part 2. Self-association and aggregation properties. *Colloids and Surfaces A: Physicochemical and Engineering Aspects* **2017,** *514*, 79-90.

61.   Ruwoldt, J.; Subramanian, S.; Simon, S.; Oschmann, H.; Sjöblom, J. Asphaltene fractionation based on adsorption onto calcium carbonate: Part 3. Effect of asphaltenes on wax crystallization. *Colloids and Surfaces A: Physicochemical and Engineering Aspects* **2018,** *554*, 129-141.

62.   Mezger, T. *The Rheology Handbook: For users of rotational and oscillatory rheometers.*; Vincentz Verlag: Hannover, 2002.

63.   Huang, Z.; Zheng, S.; Fogler, H. S. *Wax Deposition: Experimental Characterizations, Theoretical Modeling, and Field Practices*; CRC Press: Boca Raton (FL), USA, 2015.

64.   Ruwoldt, J.; Kurniawan, M.; Oschmann, H.-J. Non-linear dependency of wax appearance temperature on cooling rate. *Journal of Petroleum Science and Engineering* **2018,** *165*, 114-126.

65.   Kruka, V. R.; Cadena, E. R.; Long, T. E. Cloud-Point Determination for Crude Oils. *Journal of Petroleum Technology* **1995,** *47* (08), 681-687.

66.   Standard Test Method for Cloud Point of Petroleum Products and Liquid Fuels. In *ASTM D2500*; ASTM International, 2017.

67.   Kruka, V. R.; Cadena, E. R.; Long, T. E. Cloud-Point Determination for Crude Oils. **1995**.

68.   Becker, J. R. Paraffin-Crystal-Modifier Studies in Field and Laboratory. Society of Petroleum Engineers, 2001.

69.   Karacan, C. Ö.; Demiral, M. R. B.; Kök, M. V. Application of X-ray CT Imaging as an Alternative Tool for Cloud Point Determination. *Petroleum Science and Technology* **2000,** *18* (7-8), 835-849.

70.   Paso, K.; Kallevik, H.; Sjoblom, J. Measurement of wax appearance temperature using near-infrared (NIR) scattering. *Energy & Fuels* **2009,** *23* (10), 4988-4994.

71.   Zougari, M. I.; Sopkow, T. Introduction to Crude Oil Wax Crystallization Kinetics: Process Modeling. *Industrial & Engineering Chemistry Research* **2007,** *46* (4), 1360-1368.

72.   Alcazar-Vara, L. A.; Buenrostro-Gonzalez, E. Liquid-solid phase equilibria of paraffinic systems by DSC measurements. In *Applications of Calorimetry in a Wide Context-Differential Scanning Calorimetry, Isothermal Titration Calorimetry and Microcalorimetry*; IntechOpen, 2013.

73.   Kok, M. V.; Létoffé, J.-M.; Claudy, P.; Martin, D.; Garcin, M.; Volle, J.-L. Comparison of wax appearance temperatures of crude oils by differential scanning calorimetry, thermomicroscopy and viscometry. *Fuel* **1996,** *75* (7), 787-790.

74.   Kök, M. V.; Letoffe, J. M.; Claudy, P. DSC and Rheometry Investigations of Crude Oils. *J Therm Anal Calorim* **1999,** *56* (2), 959-965.

75.   Japper-Jaafar, A.; Bhaskoro, P. T.; Mior, Z. S. A new perspective on the measurements of wax appearance temperature: Comparison between DSC, thermomicroscopy and rheometry and the cooling rate effects. *Journal of Petroleum Science and Engineering* **2016,** *147*, 672-681.

76.   Ahmadi Khoshooei, M.; Fazlollahi, F.; Maham, Y.; Hassan, A.; Pereira-Almao, P. A review on the application of differential scanning calorimetry (DSC) to petroleum products. *J Therm Anal Calorim* **2019**.

77.   Paiva, F. L.; Calado, V. M. A.; Marchesini, F. H. On the use of Modulated Temperature Differential Scanning Calorimetry to assess wax crystallization in crude oils. *Fuel* **2017,** *202*, 216-226.

78.   Alghanduri, L. M.; Elgarni, M. M.; Daridon, J.-L.; Coutinho, J. A. P. Characterization of Libyan Waxy Crude Oils. *Energy & Fuels* **2010,** *24* (5), 3101-3107.

79.   Paso, K.; Kompalla, T.; Aske, N.; Sjöblom, J. A Quartz Crystal Microbalance Characterization of Metal-Oil Interfaces and Interactions with Wax Molecules. *Journal of Dispersion Science and Technology* **2008,** *29* (5), 775-782.

80.   Musser, B. J.; Kilpatrick, P. K. Molecular Characterization of Wax Isolated from a Variety of Crude Oils. *Energy & Fuels* **1998,** *12* (4), 715-725.

81.   Nagazi, M. Y.; Dieudonné-George, P.; Brambilla, G.; Meunier, G.; Cipelletti, L. Phase transitions in polymorphic materials probed using space-resolved diffusing wave spectroscopy. *Soft Matter* **2018,** *14* (31), 6439-6448.

82.   Zhao, Y.; Paso, K.; Sjöblom, J. Thermal behavior and solid fraction dependent gel strength model of waxy oils. *J Therm Anal Calorim* **2014,** *117* (1), 403-411.

83.   Mothé, M. G.; Perin, M.; Mothé, C. G. Comparative thermal study of heavy crude oils by DSC. *Petroleum Science and Technology* **2016,** *34* (4), 314-320.

84.   Vieira, L. C.; Buchuid, M. B.; Lucas, E. F. Effect of Pressure on the Crystallization of Crude Oil Waxes. I. Selection of Test Conditions by Microcalorimetry. *Energy & Fuels* **2010,** *24* (4), 2208-2212.

85.   Paso, K.; Braathen, B.; Viitala, T.; Aske, N.; Rønningsen, H.; Sjöblom, J. Wax Deposition Investigations with Thermal Gradient Quartz Crystal Microbalance. In *Handbook of Surface and Colloid Chemistry*; CRC Press, 2009, pp 567-584.

86.   Al-Zahrani, S. M.; Al-Fariss, T. F. A general model for the viscosity of waxy oils. *Chemical Engineering and Processing: Process Intensification* **1998,** *37* (5), 433-437.

87.   Pedersen, K. S.; Rønningsen, H. P. Effect of Precipitated Wax on ViscosityA Model for Predicting Non-Newtonian Viscosity of Crude Oils. *Energy & Fuels* **2000,** *14* (1), 43-51.

88.   Paso, K.; Silset, A.; Sørland, G.; Gonçalves, M. d. A.; Sjöblom, J. Characterization of the formation, flowability, and resolution of Brazilian crude oil emulsions. *Energy & Fuels* **2008,** *23* (1), 471-480.

89.   Rodriguez-Fabia, S.; Lopez Fyllingsnes, R.; Winter-Hjelm, N.; Norrman, J.; Paso, K. G. Influence of Measuring Geometry on Rheomalaxis of Macrocrystalline Wax–Oil Gels: Alteration of Breakage Mechanism from Adhesive to Cohesive. *Energy & Fuels* **2019,** *33* (2), 654-664.

90.   Standard Test Method for Pour Point of Petroleum Products. In *D97*: ASTM International, 2017.

91.   Winter, H. H.; Chambon, F. Analysis of Linear Viscoelasticity of a Crosslinking Polymer at the Gel Point. *Journal of Rheology* **1986,** *30* (2), 367-382.

92.   Li, Y.; Han, S.; Lu, Y.; Zhang, J. Influence of Asphaltene Polarity on Crystallization and Gelation of Waxy Oils. *Energy & Fuels* **2018,** *32* (2), 1491-1497.

93.   Tinsley, J. F.; Jahnke, J. P.; Dettman, H. D.; Prud'home, R. K. Waxy Gels with Asphaltenes 1: Characterization of Precipitation, Gelation, Yield Stress, and Morphology. *Energy & Fuels* **2009,** *23* (4), 2056-2064.

94.   Venkatesan, R.; Östlund, J.-A.; Chawla, H.; Wattana, P.; Nydén, M.; Fogler, H. S. The Effect of Asphaltenes on the Gelation of Waxy Oils. *Energy & Fuels* **2003,** *17* (6), 1630-1640.

95.   Venkatesan, R.; Singh, P.; Fogler, H. S. Delineating the Pour Point and Gelation Temperature of Waxy Crude Oils. **2004**.

96.   Bossard, F.; Moan, M.; Aubry, T. Linear and nonlinear viscoelastic behavior of very concentrated plate-like kaolin suspensions. *Journal of Rheology* **2007,** *51* (6), 1253-1270.

97.   Ruwoldt, J.; Kurniawan, M.; Humborstad Sørland, G.; Simon, S.; Sjöblom, J. Influence of wax inhibitor molecular weight: Fractionation and effect on crystallization of polydisperse waxes. *Journal of Dispersion Science and Technology* **2019**, 1-16.

98. Zhao, Y.; Paso, K.; Kumar, L.; Safieva, J.; Sariman, M. Z. B.; Sjöblom, J. Controlled Shear Stress and Controlled Shear Rate Nonoscillatory Rheological Methodologies for Gelation Point Determination. *Energy & Fuels* **2013,** *27* (4), 2025-2032.

99. Yao, B.; Li, C.; Zhang, X.; Yang, F.; Sun, G.; Zhao, Y. Performance improvement of the ethylene-vinyl acetate copolymer (EVA) pour point depressant by small dosage of the amino-functionalized polymethylsilsesquioxane (PAMSQ) microsphere. *Fuel* **2018,** *220*, 167-176.

100. Kané, M.; Djabourov, M.; Volle, J.-L.; Lechaire, J.-P.; Frebourg, G. Morphology of paraffin crystals in waxy crude oils cooled in quiescent conditions and under flow. *Fuel* **2003,** *82* (2), 127-135.

101. Chang, C.; Nguyen, Q. D.; Rønningsen, H. P. Isothermal start-up of pipeline transporting waxy crude oil. *Journal of Non-Newtonian Fluid Mechanics* **1999,** *87* (2), 127-154.

102. Petter Rønningsen, H. Rheological behaviour of gelled, waxy North Sea crude oils. *Journal of Petroleum Science and Engineering* **1992,** *7* (3–4), 177-213.

103. Dalla, L. F. R.; Soares, E. J.; Siqueira, R. N. Start-up of waxy crude oils in pipelines. *Journal of Non-Newtonian Fluid Mechanics* **2019,** *263*, 61-68.

104. Dimitriou, C. J.; McKinley, G. H.; Venkatesan, R. Rheo-PIV Analysis of the Yielding and Flow of Model Waxy Crude Oils. *Energy & Fuels* **2011,** *25* (7), 3040-3052.

105. Lee, H. S.; Singh, P.; Thomason, W. H.; Fogler, H. S. Waxy Oil Gel Breaking Mechanisms: Adhesive versus Cohesive Failure. *Energy & Fuels* **2008,** *22* (1), 480-487.

106. Ribeiro, F. S.; Souza Mendes, P. R.; Braga, S. L. Obstruction of pipelines due to paraffin deposition during the flow of crude oils. *International Journal of Heat and Mass Transfer* **1997,** *40* (18), 4319-4328.

107. Hoffmann, R.; Amundsen, L. Single-Phase Wax Deposition Experiments. *Energy & Fuels* **2010,** *24* (2), 1069-1080.

108. Soedarmo, A. A.; Daraboina, N.; Sarica, C. Microscopic Study of Wax Deposition: Mass Transfer Boundary Layer and Deposit Morphology. *Energy & Fuels* **2016,** *30* (4), 2674-2686.

109. Li, C.; Cai, J.; Yang, F.; Zhang, Y.; Bai, F.; Ma, Y.; Yao, B. Effect of asphaltenes on the stratification phenomenon of wax-oil gel deposits formed in a new cylindrical Couette device. *Journal of Petroleum Science and Engineering* **2016,** *140*, 73-84.

110. Bidmus, H.; Mehrotra, A. K. Measurement of the liquid– deposit interface temperature during solids deposition from wax– solvent mixtures under sheared cooling. *Energy & fuels* **2008,** *22* (6), 4039-4048.

111. Paso, K. G.; Fogler, H. S. Bulk Stabilization in Wax Deposition Systems. *Energy & Fuels* **2004,** *18* (4), 1005-1013.

112. Yang, F.; Cai, J.; Cheng, L.; Li, C.; Ji, Z.; Yao, B.; Zhao, Y.; Zhang, G. Development of Asphaltenes-Triggered Two-Layer Waxy Oil Gel Deposit under Laminar Flow: An Experimental Study. *Energy & Fuels* **2016,** *30* (11), 9922-9932.

113. Ruwoldt, J. Inhibitor-Wax Interactions and Wax Crystallization: New Experimental Approaches and Techniques. Ph.D, NTNU2018.

114. Xu, J.; Xing, S.; Qian, H.; Chen, S.; Wei, X.; Zhang, R.; Li, L.; Guo, X. Effect of polar/nonpolar groups in comb-type copolymers on cold flowability and paraffin crystallization of waxy oils. *Fuel* **2013,** *103*, 600-605.

115. Tinsley, J. F.; Jahnke, J. P.; Adamson, D. H.; Guo, X.; Amin, D.; Kriegel, R.; Saini, R.; Dettman, H. D.; Prud'home, R. K. Waxy Gels with Asphaltenes 2: Use of Wax Control Polymers. *Energy & Fuels* **2009,** *23* (4), 2065-2074.

116. Ruwoldt, J.; Humborstad Sørland, G.; Simon, S.; Oschmann, H.-J.; Sjöblom, J. Inhibitor-wax interactions and PPD effect on wax crystallization: New approaches for GC/MS and NMR, and comparison with DSC, CPM, and rheometry. *Journal of Petroleum Science and Engineering* **2019,** *177*, 53-68.

117. Norrman, J.; Solberg, A.; Sjöblom, J.; Paso, K. Nanoparticles for Waxy Crudes: Effect of Polymer Coverage and the Effect on Wax Crystallization. *Energy & Fuels* **2016,** *30* (6), 5108-5114.

118.   Paso, K. G.; Krückert, K. K.; Oschmann, H.-J.; Ali, H.; Sjöblom, J. PPD architecture development via polymer–crystal interaction assessment. *Journal of Petroleum Science and Engineering* **2014,** *115*, 38-49.

119.   Oliveira, G. E.; Mansur, C. R. E.; Lucas, E. F.; González, G.; de Souza, W. F. The Effect of Asphaltenes, Naphthenic Acids, and Polymeric Inhibitors on the Pour Point of Paraffins Solutions. *Journal of Dispersion Science and Technology* **2007,** *28* (3), 349-356.

120.   Pedersen, K. S.; Rønningsen, H. P. Influence of Wax Inhibitors on Wax Appearance Temperature, Pour Point, and Viscosity of Waxy Crude Oils. *Energy & Fuels* **2003,** *17* (2), 321-328.

121.   Li, L.; Xu, J.; Tinsley, J.; Adamson, D. H.; Pethica, B. A.; Huang, J. S.; Prud'homme, R. K.; Guo, X. Improvement of oil flowability by assembly of comb-type copolymers with paraffin and asphaltene. *AIChE Journal* **2012,** *58* (7), 2254-2261.

122.   Zhang, J.; Zhang, M.; Wan, J.; Li, W. Theoretical Study of the Prohibited Mechanism for Ethylene/Vinyl Acetate Co-polymers to the Wax Crystal Growth. *The Journal of Physical Chemistry B* **2008,** *112* (1), 36-43.

123.   Wu, C.; Zhang, J.-l.; Li, W.; Wu, N. Molecular dynamics simulation guiding the improvement of EVA-type pour point depressant. *Fuel* **2005,** *84* (16), 2039-2047.

124.   Zhang, J.; Wu, C.; Li, W.; Wang, Y.; Cao, H. DFT and MM calculation: the performance mechanism of pour point depressants study. *Fuel* **2004,** *83* (3), 315-326.

125.   Duffy, D.; Rodger, P. Wax inhibition with poly (octadecyl acrylate). *Physical Chemistry Chemical Physics* **2002,** *4* (2), 328-334.

126.   Chen, Z.; Wang, X.; Zhang, H.; Yang, C.; Shan, H. A Study on the Interaction of Crude Oil Waxes With Polyacrylate Pour Point Depressants by Monte Carlo Simulation. *Petroleum Science and Technology* **2014,** *32* (17), 2151-2157.

127.   Monkenbusch, M.; Schneiders, D.; Richter, D.; Willner, L.; Leube, W.; Fetters, L. J.; Huang, J. S.; Lin, M. Aggregation behaviour of PE–PEP copolymers and the winterization of diesel fuel. *Physica B: Condensed Matter* **2000,** *276-278*, 941-943.

128.   Leube, W.; Monkenbusch, M.; Schneiders, D.; Richter, D.; Adamson, D.; Fetters, L.; Dounis, P.; Lovegrove, R. Wax-Crystal Modification for Fuel Oils by Self-Aggregating Partially Crystallizable Hydrocarbon Block Copolymers. *Energy & Fuels* **2000,** *14* (2), 419-430.

129.   Ruwoldt, J.; Simon, S.; Oschmann, H.; Sjöblom, J. In *Isothermal Titration Calorimetry for Assessing Wax-Inhibitors*, Chemistry in the Oil Industry XV: Enabling Efficient Technologies Programme, Manchester (UK), 2017; Jackson, S., Ed.

130.   Ruwoldt, J.; Simon, S.; Norrman, J.; Oschmann, H.-J.; Sjöblom, J. Wax-Inhibitor Interactions Studied by Isothermal Titration Calorimetry and Effect of Wax Inhibitor on Wax Crystallization. *Energy & Fuels* **2017,** *31* (7), 6838-6847.

131.   Alcazar-Vara, L. A.; Garcia-Martinez, J. A.; Buenrostro-Gonzalez, E. Effect of asphaltenes on equilibrium and rheological properties of waxy model systems. *Fuel* **2012,** *93*, 200-212.

132.   Lei, Y.; Han, S.; Zhang, J. Effect of the dispersion degree of asphaltene on wax deposition in crude oil under static conditions. *Fuel Processing Technology* **2016,** *146*, 20-28.

133.   García, M. d. C. Crude Oil Wax Crystallization. The Effect of Heavy n-Paraffins and Flocculated Asphaltenes. *Energy & Fuels* **2000,** *14* (5), 1043-1048.

134.   García, M. d. C.; Carbognani, L. Asphaltene–Paraffin Structural Interactions. Effect on Crude Oil Stability. *Energy & Fuels* **2001,** *15* (5), 1021-1027.

135.   Yang, X.; Kilpatrick, P. Asphaltenes and Waxes Do Not Interact Synergistically and Coprecipitate in Solid Organic Deposits. *Energy & Fuels* **2005,** *19* (4), 1360-1375.

136.   Ariza-León, E.; Molina-Velasco, D.-R.; Chaves-Guerrero, A. Review of Studies on Asphaltene - Wax Interaction and the Effect thereof on Crystallization. *CT&F - Ciencia, Tecnología y Futuro* **2014,** *5*, 39-53.

137.   Kriz, P.; Andersen, S. I. Effect of Asphaltenes on Crude Oil Wax Crystallization. *Energy & Fuels* **2005,** *19* (3), 948-953.

138.   Lei, Y.; Han, S.; Zhang, J.; Bao, Y.; Yao, Z.; Xu, Y. n. Study on the Effect of Dispersed and Aggregated Asphaltene on Wax Crystallization, Gelation, and Flow Behavior of Crude Oil. *Energy & Fuels* **2014,** *28* (4), 2314-2321.

139.   Kaminski, T. J.; Fogler, H. S.; Wolf, N.; Wattana, P.; Mairal, A. Classification of Asphaltenes via Fractionation and the Effect of Heteroatom Content on Dissolution Kinetics. *Energy & Fuels* **2000,** *14* (1), 25-30.

140.   Prahl, U. Isolierung erdölstämmiger Pour Point Depressants und Untersuchung ihrer Wirkungsweise in paraffinhaltigen Fluiden. Dr.Ing., Technische Universität Clausthal2001.

141.   Orea, M.; Ranaudo, M. A.; Lugo, P.; López, L. Retention of Alkane Compounds on Asphaltenes. Insights About the Nature of Asphaltene–Alkane Interactions. *Energy & Fuels* **2016,** *30* (10), 8098-8113.

142.   Sun, W.; Wang, W.; Gu, Y.; Xu, X.; Gong, J. Study on the wax/asphaltene aggregation with diffusion limited aggregation model. *Fuel* **2017,** *191*, 106-113.

143.   Drelich, J.; Fang, C.; White, C. L. Measurement of interfacial tension in fluid-fluid systems. In *Encyclopedia of Surface and Colloid Science*; Marcel Dekker, 2002, pp 3152-3166.

144.   Manning, C. D.; Scriven, L. E. On interfacial tension measurement with a spinning drop in gyrostatic equilibrium. **1977,** *48* (12), 1699-1705.

145.   Vonnegut, B. Rotating Bubble Method for the Determination of Surface and Interfacial Tensions. **1942,** *13* (1), 6-9.

146.   Christov, N. C.; Danov, K. D.; Kralchevsky, P. A.; Ananthapadmanabhan, K. P.; Lips, A. Maximum Bubble Pressure Method: Universal Surface Age and Transport Mechanisms in Surfactant Solutions. *Langmuir* **2006,** *22* (18), 7528-7542.

147.   Fainerman, V. B.; Mys, V. D.; Makievski, A. V.; Petkov, J. T.; Miller, R. Dynamic surface tension of micellar solutions in the millisecond and submillisecond time range. *Journal of Colloid and Interface Science* **2006,** *302* (1), 40-46.

148.   Eftekhardadkhah, M.; Reynders, P.; Øye, G. Dynamic adsorption of water soluble crude oil components at air bubbles. *Chemical Engineering Science* **2013,** *101*, 359-365.

149.   Eastoe, J.; Dalton, J. S. Dynamic surface tension and adsorption mechanisms of surfactants at the air–water interface. *Adv. Colloid Interface Sci.* **2000,** *85* (2–3), 103-144.

150.   Chang, C.-H.; Franses, E. I. Adsorption dynamics of surfactants at the air/water interface: a critical review of mathematical models, data, and mechanisms. *Colloids Surf., A* **1995,** *100* (0), 1-45.

151.   Pradilla, D.; Simon, S.; Sjöblom, J. Mixed interfaces of asphaltenes and model demulsifiers part I: Adsorption and desorption of single components. *Colloids and Surfaces A: Physicochemical and Engineering Aspects* **2015,** *466* (0), 45-56.

152.   Pradilla, D.; Simon, S.; Sjöblom, J. Mixed Interfaces of Asphaltenes and Model Demulsifiers, Part II: Study of Desorption Mechanisms at Liquid/Liquid Interfaces. *Energy Fuels* **2015,** *29* (9), 5507-5518.

153.   Rane, J. P.; Zarkar, S.; Pauchard, V.; Mullins, O. C.; Christie, D.; Andrews, A. B.; Pomerantz, A. E.; Banerjee, S. Applicability of the Langmuir Equation of State for Asphaltene Adsorption at the Oil–Water Interface: Coal-Derived, Petroleum, and Synthetic Asphaltenes. *Energy & Fuels* **2015,** *29* (6), 3584-3590.

154.   Sauerer, B.; Stukan, M.; Buiting, J.; Abdallah, W.; Andersen, S. Dynamic Asphaltene-Stearic Acid Competition at the Oil–Water Interface. *Langmuir* **2018,** *34* (19), 5558-5573.

155.   Mullins, O. C.; Sabbah, H.; Eyssautier, J.; Pomerantz, A. E.; Barré, L.; Andrews, A. B.; Ruiz-Morales, Y.; Mostowfi, F.; McFarlane, R.; Goual, L.; Lepkowicz, R.; Cooper, T.; Orbulescu, J.; Leblanc, R. M.; Edwards, J.; Zare, R. N. Advances in Asphaltene Science and the Yen–Mullins Model. *Energy & Fuels* **2012,** *26* (7), 3986-4003.

156.   Horváth-Szabó, G.; Masliyah, J. H.; Elliott, J. A. W.; Yarranton, H. W.; Czarnecki, J. Adsorption isotherms of associating asphaltenes at oil/water interfaces based on the dependence of interfacial tension on solvent activity. *Journal of Colloid and Interface Science* **2005,** *283* (1), 5-17.

157.   Ward, A. F. H.; Tordai, L. Time Dependence of Boundary Tensions of Solutions I. The Role of Diffusion in Time Effects. *The Journal of Chemical Physics* **1946,** *14* (7), 453-461.

158.   Fainerman, V. B.; Makievski, A. V.; Miller, R. The analysis of dynamic surface tension of sodium alkyl sulphate solutions, based on asymptotic equations of adsorption kinetic theory. *Colloids and Surfaces A: Physicochemical and Engineering Aspects* **1994,** *87* (1), 61-75.

159.   Cagna, A.; Esposito, G.; Quinquis, A.-S.; Langevin, D. On the reversibility of asphaltene adsorption at oil-water interfaces. *Colloids and Surfaces A: Physicochemical and Engineering Aspects* **2018,** *548*, 46-53.

160.   Jeribi, M.; Almir-Assad, B.; Langevin, D.; Hénaut, I.; Argillier, J. F. Adsorption Kinetics of Asphaltenes at Liquid Interfaces. *Journal of Colloid and Interface Science* **2002,** *256* (2), 268-272.

161.   Ferri, J. K.; Gorevski, N.; Kotsmar, C.; Leser, M. E.; Miller, R. Desorption kinetics of surfactants at fluid interfaces by novel coaxial capillary pendant drop experiments. *Colloids Surf., A* **2008,** *319* (1–3), 13-20.

162.   Kotsmár, C.; Grigoriev, D. O.; Makievski, A. V.; Ferri, J. K.; Krägel, J.; Miller, R.; Möhwald, H. Drop profile analysis tensiometry with drop bulk exchange to study the sequential and simultaneous adsorption of a mixed β-casein /C12DMPO system. *Colloid Polym. Sci.* **2008,** *286* (8), 1071-1077.

163.   Miller, R.; Ferri, J.; Javadi, A.; Krägel, J.; Mucic, N.; Wüstneck, R. Rheology of interfacial layers. *Colloid & Polymer Science* **2010,** *288* (9), 937-950.

164.   Masschaele; Kasper; Vandebril; Steven; Vermant; Jan; Basavaraj, M. Interfacial Rheology. In *Rheology volume 1*, Gallegos, C., Ed.; Eolss Publishers Co. Ltd.: United Kingdom, 2010, pp 418-438.

165.   Strassner, J. E. Effect of pH on Interfacial Films and Stability of Crude Oil-Water Emulsions. *SPE-1939-PA* **1968,** *20* (03), 303-312.

166.   Erni, P.; Fischer, P.; Windhab, E. J.; Kusnezov, V.; Stettin, H.; Läuger, J. Stress- and strain controlled measurments of interfacial shear viscosity and viscolelasticity at liquid/liquid and gas/liquid interfaces. *Rew. Sci. Instrum.* **2003,** *74* (11), 4916-4924.

167.   Krägel, J.; Derkatch, S. R. Interfacial shear rheology. *Current Opinion in Colloid & Interface Science* **2010,** *15* (4), 246-255.

168.   Langevin, D. Surface shear rheology of monolayers at the surface of water. *Advances in Colloid and Interface Science* **2014,** *207*, 121-130.

169.   Fan, Y.; Simon, S.; Sjoblom, J. Interfacial shear rheology of asphaltenes at oil-water interface and its relation to emulsion stability: Influence of concentration, solvent aromaticity and nonionic surfactant. *Colloids Surf., A* **2010,** *366* (1-3), 120-128.

170.   Mohammed, R. A.; Bailey, A. I.; Luckham, P. F.; Taylor, S. E. Dewatering of crude oil emulsions 1. Rheological behaviour of the crude oil—water interface. *Colloids and Surfaces A: Physicochemical and Engineering Aspects* **1993,** *80* (2–3), 223-235.

171.   Spiecker, P. M.; Kilpatrick, P. K. Interfacial Rheology of Petroleum Asphaltenes at the Oil-Water Interface. *Langmuir* **2004,** *20* (10), 4022-4032.

172.   Samaniuk, J. R.; Hermans, E.; Verwijlen, T.; Pauchard, V.; Vermant, J. Soft-Glassy Rheology of Asphaltenes at Liquid Interfaces. *Journal of Dispersion Science and Technology* **2015,** *36* (10), 1444-1451.

173.   Vandebril, S.; Franck, A.; Fuller, G.; Moldenaers, P.; Vermant, J. A double wall-ring geometry for interfacial shear rheometry. *Rheol. Acta* **2010,** *49* (2), 131-144.

174.   Acevedo, S.; Escobar, G.; Gutierrez, L. B.; Rivas, H.; Gutierrez, X. Interfacial rheological studies of extra-heavy crude oils and asphaltenes: Role of the dispersion effect of resins in the adsorption of asphaltenes at the interface of water-in-crude oil emulsions. *Colloids and Surfaces A: Physicochemical and Engineering Aspects* **1993,** *71* (1), 65-71.

175.   Simon, S.; Subramanian, S.; Gao, B.; Sjöblom, J. Interfacial Shear Rheology of Gels Formed at the Oil/Water Interface by Tetrameric Acid and Calcium Ion: Influence of Tetrameric Acid Structure and Oil Composition. *Ind. Eng. Chem. Res.* **2015,** *54* (35), 8713-8722.

176.   Nordgård, E. L.; Simon, S.; Sjöblom, J. Interfacial Shear Rheology of Calcium Naphthenate at the Oil/Water Interface and the Influence of pH, Calcium and in Presence of a Model Monoacid. *J. Dispersion Sci. Technol.* **2012,** *33* (7), 1083-1092.

177.   Bertelli, J. N.; Dip, R. M. M.; Pires, R. V.; Albuquerque, F. C.; Lucas, E. F. Shear Rheology Using De Noüy Ring To Evaluate Formation and Inhibition of Calcium Naphthenate at the Water/Oil Interface. *Energy Fuels* **2014,** *28* (3), 1726-1735.

178.   Ravera, F.; Loglio, G.; Kovalchuk, V. I. Interfacial dilational rheology by oscillating bubble/drop methods. *Current Opinion in Colloid & Interface Science* **2010,** *15* (4), 217-228.

179.   Harbottle, D.; Chen, Q.; Moorthy, K.; Wang, L.; Xu, S.; Liu, Q.; Sjoblom, J.; Xu, Z. Problematic Stabilizing Films in Petroleum Emulsions: Shear Rheological Response of Viscoelastic Asphaltene Films and the Effect on Drop Coalescence. *Langmuir* **2014,** *30* (23), 6730-6738.

180.   Ligiero, L. M.; Dicharry, C.; Passade-Boupat, N.; Bouyssiere, B.; Lalli, P. M.; Rodgers, R. P.; Barrère-Mangote, C.; Giusti, P.; Bouriat, P. Characterization of Crude Oil Interfacial Material Isolated by the Wet Silica Method. Part 2: Dilational and Shear Interfacial Properties. *Energy & Fuels* **2017,** *31* (2), 1072-1081.

181.   Baugh, T. D.; Wolf, N. O.; Mediaas, H.; Vindstad, J. E.; Grande, K. Characterization of a Calcium Naphthanate Deposit - The ARN Acid Discovery. *Prepr. - Am. Chem. Soc., Div. Pet. Chem.* **2004,** *49* (3), 274-276.

182.   Lutnaes, B. F.; Brandal, O.; Sjoblom, J.; Krane, J. Archaeal C80 Isoprenoid Tetraacids Responsible for Naphthenate Deposition in Crude Oil Processing. *Org. Biomol. Chem.* **2006,** *4* (4), 616-620.

183.   Simon, S.; Nordgård, E.; Bruheim, P.; Sjöblom, J. Determination of C80 Tetra-Acid Content in Calcium Naphthenate Deposits. *J. Chromatogr., A* **2008,** *1200* (2), 136-143.

184.   Vindstad, J. E.; Grande, K. V.; Høvik, K. M.; Kummernes, H.; Mediaas, H. In *Calcium Naphthenate Management*, 8th International Conference on Petroleum Phase Behavior and Fouling, Pau (France), June 10-14 2007.

185.   Chang, C.-C.; Nowbahar, A.; Mansard, V.; Williams, I.; Mecca, J.; Schmitt, A. K.; Kalantar, T. H.; Kuo, T.-C.; Squires, T. M. Interfacial Rheology and Heterogeneity of Aging Asphaltene Layers at the Water–Oil Interface. *Langmuir* **2018,** *34* (19), 5409-5415.

186.   Reichert, M. D.; Alvarez, N. J.; Brooks, C. F.; Grillet, A. M.; Mondy, L. A.; Anna, S. L.; Walker, L. M. The importance of experimental design on measurement of dynamic interfacial tension and interfacial rheology in diffusion-limited surfactant systems. *Colloids and Surfaces A: Physicochemical and Engineering Aspects* **2015,** *467*, 135-142.

187.   Freer, E. M.; Wong, H.; Radke, C. J. Oscillating drop/bubble tensiometry: effect of viscous forces on the measurement of interfacial tension. *Journal of Colloid and Interface Science* **2005,** *282* (1), 128-132.

188.   Alexandrov, N. A.; Marinova, K. G.; Gurkov, T. D.; Danov, K. D.; Kralchevsky, P. A.; Stoyanov, S. D.; Blijdenstein, T. B. J.; Arnaudov, L. N.; Pelan, E. G.; Lips, A. Interfacial layers from the protein HFBII hydrophobin: Dynamic surface tension, dilatational elasticity and relaxation times. *Journal of Colloid and Interface Science* **2012,** *376* (1), 296-306.

189.   Ferri, J. K.; Fernandes, P. A. L.; McRuiz, J. T.; Gambinossi, F. Elastic nanomembrane metrology at fluid–fluid interfaces using axisymmetric drop shape analysis with anisotropic surface tensions: deviations from Young–Laplace equation. *Soft Matter* **2012,** *8* (40), 10352-10359.

190.   Bouriat, P.; El Kerri, N.; Graciaa, A.; Lachaise, J. Properties of a Two-Dimensional Asphaltene Network at the Water/Cyclohexane Interface Deduced from Dynamic Tensiometry. *Langmuir* **2004,** *20* (18), 7459-7464.

191.   Freer, E. M.; Radke, C. J. RELAXATION OF ASPHALTENES AT THE TOLUENE/WATER INTERFACE: DIFFUSION EXCHANGE AND SURFACE REARRANGEMENT. *The Journal of Adhesion* **2004,** *80* (6), 481-496.

192.	Quintero, C., G.; Noïk, C.; Dalmazzone, C.; Grossiord, J., L. Formation Kinetics and Viscoelastic Properties of Water/Crude Oil Interfacial Films *Oil & Gas Science and Technology - Rev. IFP* **2009,** *64* (5), 607-616.

193.	Chambon, F.; Winter, H. H. Linear Viscoelasticity at the Gel Point of a Crosslinking PDMS with Imbalanced Stoichiometry. *Journal of Rheology* **1987,** *31* (8), 683-697.

194.	Lucassen, J.; Van Den Tempel, M. Dynamic measurements of dilational properties of a liquid interface. *Chem. Eng. Sci.* **1972,** *27* (6), 1283-1291.

195.	Nenningsland, A. L.; Simon, S.; Sjöblom, J. Influence of Interfacial Rheological Properties on Stability of Asphaltene-Stabilized Emulsions. *Journal of Dispersion Science and Technology* **2013,** *35* (2), 231-243.

196.	Sztukowski, D. M.; Yarranton, H. W. Rheology of Asphaltene–Toluene/Water Interfaces. *Langmuir* **2005,** *21* (25), 11651-11658.

197.	Roux, J. N.; Broseta, D.; Deme, B. SANS Study of Asphaltene Aggregation: Concentration and Solvent Quality Effects. *Langmuir* **2001,** *17* (16), 5085-5092.

198.	Simon, S.; Knudsen, K. D.; Nordgård, E.; Reisen, C.; Sjöblom, J. Aggregation of tetrameric acids in aqueous media studied by small-angle neutron scattering. *J. Colloid Interface Sci.* **2013,** *394* (0), 277-283.

199.	Verruto, V. J.; Kilpatrick, P. K. Water-in-Model Oil Emulsions Studied by Small-Angle Neutron Scattering: Interfacial Film Thickness and Composition. *Langmuir* **2008,** *24* (22), 12807-12822.

200.	Jestin, J.; Simon, S.; Zupancic, L.; Barre, L. A Small Angle Neutron Scattering Study of the Adsorbed Asphaltene Layer in Water-in-Hydrocarbon Emulsions: Structural Description Related to Stability. *Langmuir* **2007,** *23* (21), 10471-10478.

201.	Alvarez, G.; Jestin, J.; Argillier, J. F.; Langevin, D. Small-Angle Neutron Scattering Study of Crude Oil Emulsions: Structure of the Oil–Water Interfaces. *Langmuir* **2009,** *25* (7), 3985-3990.

202.	Taylor, A.; Dunne, M.; Bennington, S.; Ansell, S.; Gardner, I.; Norreys, P.; Broome, T.; Findlay, D.; Nelmes, R. A Route to the Brightest Possible Neutron Source? **2007,** *315* (5815), 1092-1095.

203.	Espinat, D. Application of Light, X-Ray and Neutron Diffusion Techniques to the Study of Colloidal Systems. *Revue de l'Institut Francais du Petrole* **1990,** *45*, 595-820.

204.	Sears, V. F. Neutron scattering lengths and cross sections. *Neutron News* **1992,** *3* (3), 26-37.

205.	Neff, J.; Lee, K.; DeBlois, E. M. Produced Water: Overview of Composition, Fates, and Effects. In *Produced Water - Environmental Risks and Advances in Mitigation Technologies*, Lee, K.; Neff, J., Eds.; Springer New York Dordrecht Heidelberg London, 2011, pp 3-54.

206.	Igunnu, E. T.; Chen, G. Z. Produced water treatment technologies. *International Journal of Low-Carbon Technologies* **2012,** *9* (3), 157-177.

207.	Fakhru'l-Razi, A.; Pendashteh, A.; Abdullah, L. C.; Biak, D. R. A.; Madaeni, S. S.; Abidin, Z. Z. Review of technologies for oil and gas produced water treatment. *Journal of Hazardous Materials* **2009,** *170* (2), 530-551.

208.	Bringedal, B.; Ingebretsen, T.; Haugen, K. Subsea Separation and Reinjection of Produced Water, OTC-10967-MS. In *Offshore Technology Conference*; Offshore Technology Conference: Houston, Texas, 1999, p 7.

209.	Auflem, I. H.; Kallevik, H.; Westvik, A.; Sjoblom, J. Influence of pressure and solvency on the separation of water-in-crude-oil emulsions from the North Sea. *J Petrol Sci Eng* **2001,** *31* (1), 1-12.

210.	Ronningsen, H. P.; Sjoblom, J.; Mingyuan, L. Water-in-Crude Oil-Emulsions from the Norwegian Continental-Shelf .11. Aging of Crude Oils and Its Influence on the Emulsion Stability. *Colloids and Surfaces a-Physicochemical and Engineering Aspects* **1995,** *97* (2), 119-128.

211.	Walstra, P. Principles of emulsion formation. *Chemical Engineering Science* **1993,** *48* (2), 333-349.

212.	McClements, D. *Food Emulsions, 2nd Edition* CRC Press: Boca Raton, 2005.

213.	Walstra, P.; Smulder, P. E. A. Emulsion formation. In *Modern aspects of emulsion science*, Binks, B. P., Ed.; The Royal Society of Chemistry: Cmbridge, UK, 1998, pp 56-99.

214.   Grace, H. P. Dispersion Phenomena in High Viscosity Immiscible Fluid Ssystems and Application of Static Mixers as Dispersion Devices in Such Systems. *Chemical Engineering Communications* **1982,** *14* (3-6), 225-277.

215.   Eley, D. D.; Hey, M. J.; Symonds, J. D. Emulsions of water in asphaltene-containing oils 1. Droplet size distribution and emulsification rates. *Colloids and Surfaces* **1988,** *32*, 87-101.

216.   Jokela, P.; Fletcher, P. D. I.; Aveyard, R.; Lu, J.-R. The use of computerized microscopic image analysis to determine emulsion droplet size distributions. *Journal of Colloid and Interface Science* **1990,** *134* (2), 417-426.

217.   Moradi, M.; Alvarado, V.; Huzurbazar, S. Effect of Salinity on Water-in-Crude Oil Emulsion: Evaluation through Drop-Size Distribution Proxy. *Energy & Fuels* **2011,** *25* (1), 260-268.

218.   Lu, Y.; Kang, W.; Jiang, J.; Chen, J.; Xu, D.; Zhang, P.; Zhang, L.; Feng, H.; Wu, H. Study on the stabilization mechanism of crude oil emulsion with an amphiphilic polymer using the β-cyclodextrin inclusion method. *RSC Advances* **2017,** *7* (14), 8156-8166.

219.   ASTM. Standard Test Methods for Water in Crude Oils by Coulometric Karl Fischer Titration. 2000; Vol. D 4928-00.

220.   Xu, B.; Kang, W.; Wang, X.; Meng, L. Influence of Water Content and Temperature on Stability of W/O Crude Oil Emulsion. *Petroleum Science and Technology* **2013,** *31* (10), 1099-1108.

221.   Frising, T.; Noïk, C.; Dalmazzone, C. The Liquid/Liquid Sedimentation Process: From Droplet Coalescence to Technologically Enhanced Water/Oil Emulsion Gravity Separators: A Review. *Journal of Dispersion Science and Technology* **2006,** *27* (7), 1035 - 1057.

222.   van Dick, J.; Havre, T. E.; Oschmann, H.-J. Monitoring the Demulsification of Crude Oil Emulsions by Using Conductivity Measurements. In *Emulsions and Emulsion Stability*, 2nd ed.; Sjöblom, J., Ed.; CRC Press: Boca Raton, FL, 2006, pp 651-62.

223.   Brocart, B.; Hurtevent, C. Flow Assurance Issues and Control with Naphthenic Oils. *J. Dispersion Sci. Technol.* **2008,** *29* (10), 1496 - 1504.

224.   Bukhari, S. F. A.; Yang, W. Multi-interface Level Sensors and New Development in Monitoring and Control of Oil Separators. *Sensors (Basel)* **2006,** *6* (4), 380-389.

225.   Yang, W. Q.; Brant, M. R.; Beck, M. S. A multi-interface level measurement system using a segmented capacitance sensor for oil separators. *Measurement Science and Technology* **1994,** *5* (9), 1177-1180.

226.   Balinov, B.; Urdahl, O.; Söderman, O.; Sjöblom, J. Characterization of water-in-crude oil emulsions by the NMR self-diffusion technique. *Colloids and Surfaces A: Physicochemical and Engineering Aspects* **1994,** *82* (2), 173-181.

227.   Peña, A. A.; Hirasaki, G. J. Enhanced characterization of oilfield emulsions via NMR diffusion and transverse relaxation experiments. *Advances in Colloid and Interface Science* **2003,** *105* (1-3), 103-150.

228.   Jiang, T.; Hirasaki, G.; Miller, C.; Moran, K.; Fleury, M. Diluted Bitumen Water-in-Oil Emulsion Stability and Characterization by Nuclear Magnetic Resonance (NMR) Measurements *Energy & Fuels* **2007,** *21* (3), 1325-1336.

229.   Opedal, N. v. d. T.; Sørland, G.; Sjöblom, J. Methods for Droplet Size Distribution Determination of Water-in-oil Emulsions using Low-Field NMR. *diffusion-fundamentals.org, available at http://www.uni-leipzig.de/diffusion/* **2009,** *9* (7), 1-29.

230.   Opedal, N. v. d. T.; Sørland, G.; Sjöblom, J. Emulsion Stability Studied by Nuclear Magnetic Resonance (NMR). *Energy & Fuels* **2010,** *24* (6), 3628-3633.

231.   Sandnes, R.; Simon, S.; Sjöblom, J.; Sørland, G. H. Optimization and Validation of Low Field Nuclear Magnetic Resonance Sequences to Determine Low Water Contents and Water Profiles in W/O Emulsions. *Colloids and Surfaces A: Physicochemical and Engineering Aspects* **2014,** *441*, 441-448.

232.   Sørland, G. H. *Dynamic Pulsed-Field-Gradient NMR*; Springer Berlin Heidelberg: Berlin, Heidelberg, 2014.

233.	Hjartnes, T. N.; Sørland, G. H.; Simon, S.; Sjöblom, J. Demulsification of Crude Oil Emulsions Tracked by Pulsed Field Gradient (PFG) Nuclear Magnetic Resonance (NMR). Part I: Chemical Demulsification. *Industrial & Engineering Chemistry Research* **2019,** *58* (6), 2310-2323.

234.	Grimes, B. A.; Dorao, C. A.; Opedal, N. V. D. T.; Kralova, I.; Sørland, G. H.; Sjöblom, J. Population Balance Model for Batch Gravity Separation of Crude Oil and Water Emulsions. Part II: Comparison to Experimental Crude Oil Separation Data. *Journal of Dispersion Science and Technology* **2012,** *33* (4), 591-598.

235.	Whitesides, G. M. The origins and the future of microfluidics. *Nature* **2006,** *442* (7101), 368-373.

236.	David J. Beebe; Glennys A. Mensing, a.; Walker, G. M. Physics and Applications of Microfluidics in Biology. **2002,** *4* (1), 261-286.

237.	Teh, S.-Y.; Lin, R.; Hung, L.-H.; Lee, A. P. Droplet microfluidics. *Lab on a Chip* **2008,** *8* (2), 198-220.

238.	Dudek, M.; Bertheussen, A.; Dumaire, T.; Øye, G. Microfluidic tools for studying coalescence of crude oil droplets in produced water. *Chemical Engineering Science* **2018,** *191*, 448-458.

239.	Dudek, M. Produced Water Quality and Microfluidic Methods for Studying Drop-Drop and Drop-Bubble Interactions in Produced Water. PhD, Norwegian University of Science and Technology NTNU, June 2018 2018.

240.	Dudek, M.; Muijlwijk, K.; Schroën, K.; Øye, G. The effect of dissolved gas on coalescence of oil drops studied with microfluidics. *Journal of Colloid and Interface Science* **2018,** *528*, 166-173.

241.	Dudek, M.; Øye, G. Microfluidic Study on the Attachment of Crude Oil Droplets to Gas Bubbles. *Energy & Fuels* **2018,** *32* (10), 10513-10521.

242.	Lin, Y.-J.; Perrard, A.; Biswal, S. L.; Hill, R. M.; Trabelsi, S. Microfluidic Investigation of Asphaltenes-Stabilized Water-in-Oil Emulsions. *Energy & Fuels* **2018,** *32* (4), 4903-4910.

243.	Nowbahar, A.; Whitaker, K. A.; Schmitt, A. K.; Kuo, T.-C. Mechanistic Study of Water Droplet Coalescence and Flocculation in Diluted Bitumen Emulsions with Additives Using Microfluidics. *Energy & Fuels* **2017,** *31* (10), 10555-10565.

244.	Chen, D.; Cardinaels, R.; Moldenaers, P. Effect of Confinement on Droplet Coalescence in Shear Flow. *Langmuir* **2009,** *25* (22), 12885-12893.

245.	Vananroye, A.; Van Puyvelde, P.; Moldenaers, P. Effect of Confinement on Droplet Breakup in Sheared Emulsions. *Langmuir* **2006,** *22* (9), 3972-3974.